8. van der Loo J, Hanenberg H, Cooper R, Luo F-Y, Lazaridis E, Williams D. Nonobese diabetic/severe combined immunodeficiency (NOD/S-CID) mouse as a model system to study the engraftment and mobilization of human peripheral blood stem cells. Blood. 1998;92:2556–2570.
9. Roncarolo M, Carballido J, Rouleau M, Namikawa R, de Vries J. Human T-and B-cell functions in SCID-hu mice. Semin Immunol. 1996;8:207–213.
10. McCune J, Namikawa R, Kaneshima H, Shultz L, Lieberman M, Weissman I. The SCID-hu mouse: murine model for the analysis of human hematolymphoid differentiation and function. Science. 1988; 241:1632–1639.
11. Novelli E, Ramirez M, Leung W, Civin C. Human hematopoietic stem/progenitor cells generate CD5+ B lymphoid cells in NOD/SCID mice. Stem Cells. 1999;17:242–252.
12. Ito M, Hiramatsu H, Kobayashi K, et al. NOD/SCID/gamma(c)(null) mouse: an excellent recipient mouse model for engraftment of human cells. Blood. 2002;100:3175–3182.
13. Ito M, Kobayashi K, Nakahata T. NOD/Shi-scid IL2rgamma(null) (NOG) mice more appropriate for humanized mouse models. Curr Top Microbiol Immunol. 2008;324:53–76.
14. Kametani Y, Shiina M, Katano I, et al. Development of human-human hybridoma from anti-Her-2 peptide-producing B cells in immunized NOG mouse. Exp Hematol. 2006;34:1240–1248.
15. Matsumura T, Kametani Y, Ando K, et al. Functional CD5+ B cells develop predominantly in the spleen of NOD/SCID/gammac(null) (NOG) mice transplanted either with human umbilical cord blood, bone marrow, or mobilized peripheral blood CD34+ cells. Exp Hematol. 2003;34:1240–1248.
16. Saito Y, Kametani Y, Hozumi K, et al. Reconstitution of functional human B lymphocytes in NOD/SCID mice engrafted with ex vivo expanded CD34(+) cord blood cells. Int Immunol. 2002;30:1036–1043.
17. Ito R, Shiina M, Saito Y, Tokuda Y, Kametani Y, Habu S. Antigen-specific antibody production of human B cells in NOG mice reconstituted with the human immune system. Curr Top Microbiol Immunol. 2008;324:95–107.
18. Mansfield K. Marmoset models commonly used in biomedical research. Comp Med. 2003;53:383–392.
19. Mansfield K, Tardif S, Eichler E. White paper for complete sequencing of the common marmoset (Callithrix jacchus). 2004. Available at: http://www.genome.gov/Pages/Research/Sequencing/SeqProposals/MarmosetSeq.pdf. Accessed September 18, 2009.
20. Hibino H, Tani K, Ikebuchi K, et al. The common marmoset as a target preclinical primate model for cytokine and gene therapy studies. Blood. 2008;93:2839–2848.
21. Genain C, Abel K, Belmar N, et al. Late complications of immune deviation therapy in a nonhuman primate. Science. 1996;274:2054–2057.
22. Genain C, Hauser S. Experimental allergic encephalomyelitis in the new world monkey Callithrix jacchus. Immunol Rev. 2001;183:159–192.
23. LaBonte J, Babcock G, Patel T, Sodroski J. Blockade of HIV-1 infection of new world monkey cells occurs primarily at the stage of virus entry. J Exp Med. 2002;431:431–445.
24. Einspanier A, Lieder K, Bruns A, Husen B, Thole H, Simon C. Induction of endometriosis in the marmoset monkey (Callithrix jacchus). Mol Hum Reprod. 2006;12:291–299.
25. Massacesi L, Genain C, Lee-Parritz D, Letvin N, Canfield D, Hauser S. Active and passively induced experimental autoimmune encephalomyelitis in common marmosets: a new model for multiple sclerosis. Ann Neurol. 1995;37:519–530.
26. 't Hart B, Laman J, Bauer J, Blezer E, van Kooyk Y, Hintzen R. Modelling of multiple sclerosis: lessons learned in a non-human primate. Lancet Neurol. 2004;3:588–597.
27. Sasaki E, Suemizu H, Shimada A, et al. Generation of transgenic non-human primates with germline transmission. Nature. 2009;459:515–516.
28. Kohu K, Yamabe E, Matsuzawa A, et al. Comparison of 30 immunity-related genes from the common marmoset with orthologues from human and mouse. Tohoku J Exp Med. 2008;215:167–180.
29. Izawa K, Tani K, Nakazaki Y, et al. Hematopoietic activity of common marmoset CD34 cells isolated by a novel monoclonal antibody MA24. Exp Hematol. 2004;32:843–851.
30. Brok H, Hornby R, Griffiths G, Scott L, Hart B. An extensive monoclonal antibody panel for the phenotyping of leukocyte subsets in the common marmoset and the cotton-top tamarin. Cytometry. 2001;45: 294–303.
31. Marchler-Bauer A, Anderson J, Cherukuri P, et al. CDD: a conserved domain database for protein classification. Nucleic Acids Res. 2005; 33:192–196.
32. Song Y, Liu F, Zhang G, Liu D. Hydrodynamics-based transfection: simple and efficient method for introducing and expressing transgenes in animals by intravenous injection of DNA. Methods Enzymol. 2002; 246:92–105.
33. Ito R, Maekawa S, Kawai K, et al. Novel monoclonal antibodies recognizing different subsets of lymphocytes from the common marmoset (Callithrix jacchus). Immunol Lett. 2008;121:116–122.
34. McFarland H, Lobito A, Johnson M, et al. Effective antigen-specific immunotherapy in the marmoset model of multiple sclerosis. J Immunol. 2001;166:2116–2121.
35. Accardo-Palumbo A, Ferrante A, Cadelo M, et al. The level of Granzyme A is elevated in the plasma and in the Vgamma9/Vdelta2 T cell culture supernatants with active Behger's disease. Clin Exp Rheumatol. 2004;22(Suppl 34):S45–S49.
36. Amu S, Tarkowski A, Dorner T, Bokarewa M, Brisslert M. The human immunomodulatory CD25+ B cell population belongs to the memory B cell pool. Scand J Immunol. 2007;66:77–86.
37. Brisslert M, Bokarewa M, Larsson P, Wing K, Collins L, Tarkowski A. Phenotypic and functional characterization of human CD25+ B cells. Immunology. 2006;117:548–557.
38. Papayannopoulou B, Brice M, Broudy V, Zsebo K. Isolation of c-kit receptor-expressing cells from bone marrow, peripheral blood, and fetal liver: functional properties and composite antigenic profile. Blood. 1991;78:1403–1412.
39. Hogan C, Shpall E, McNulty O, et al. Engraftment and development of human CD34(+)-enriched cells from umbilical cord blood in NOD/LtSz-scid/scid mice. Blood. 1997;90:85–96.
40. Greiner D, Hesselton R, Shultz L. SCID mouse models of human stem cell engraftment. Stem Cells. 1998;16:166–177.
41. Wermann K, Fruehauf S, Haas R, Zeller W. Human-mouse xenografts in stem cell research. J Hematother. 1996;5:379–390.
42. Galy A, Morel F, Hill B, Chen B. Hematopoietic progenitor cells of lymphocytes and dendritic cell. J Immunother. 1998;21:132–141.
43. Okada S, Nakauchi H, Nagayoshi K, Nishikawa S, Miura Y, Suda T. In vivo and in vitro stem cell function of c-kit- and Sca-1-positive murine hematopoietic cells. Blood. 1992;80:3044–3050.

Vaccine 27 (2009) 7116–7124

Contents lists available at ScienceDirect

Vaccine

journal homepage: www.elsevier.com/locate/vaccine

A genetically engineered adenovirus vector targeted to CD40 mediates transduction of canine dendritic cells and promotes antigen-specific immune responses *in vivo*

Erin E. Thacker[a], Masaharu Nakayama[a], Bruce F. Smith[g,h], R. Curtis Bird[h], Zhanat Muminova[e], Theresa V. Strong[c,d,e], Laura Timares[c,f], Nikolay Korokhov[i], Ann Marie O'Neill[g], Tanja D. de Gruijl[j], Joel N. Glasgow[a,b,d], Kenzaburo Tani[k], David T. Curiel[a,c,d,*]

[a] Division of Human Gene Therapy, Departments of Medicine, Obstetrics and Gynecology, Pathology, Surgery, Birmingham, AL 35294, United States
[b] Division of Cardiovascular Disease, University of Alabama at Birmingham, Birmingham, AL 35294, United States
[c] Comprehensive Cancer Center, University of Alabama at Birmingham, Birmingham, AL 35294, United States
[d] Gene Therapy Center, University of Alabama at Birmingham, Birmingham, AL 35294, United States
[e] Division of Hematology/Oncology, Department of Medicine, University of Alabama at Birmingham, Birmingham, AL 35294, United States
[f] Department of Dermatology, The UAB Skin Diseases Research Center, University of Alabama at Birmingham, Birmingham, AL 35294, United States
[g] Scott-Ritchey Research Center, Auburn University, Auburn, AL 36849, United States
[h] Department of Pathobiology, Auburn University, Auburn, AL 36849, United States
[i] VectorLogics, Inc., Birmingham, AL 35294, United States
[j] Division of Immunotherapy, Department of Medical Oncology, VU University Medical Center, Amsterdam, The Netherlands
[k] Division of Molecular and Clinical Genetics, Medical Institution of Bioregulation, Kyushu University, Fukuoka, Japan

ARTICLE INFO

Article history:
Received 26 August 2008
Received in revised form 2 September 2009
Accepted 16 September 2009
Available online 26 September 2009

Keywords:
Cancer immunotherapy
Adenovirus
Dendritic cell
Dog
Vaccine

ABSTRACT

Targeting viral vectors encoding tumor-associated antigens to dendritic cells (DCs) *in vivo* is likely to enhance the effectiveness of immunotherapeutic cancer vaccines. We have previously shown that genetic modification of adenovirus (Ad) 5 to incorporate CD40 ligand (CD40L) rather than native fiber allows selective transduction and activation of DCs *in vitro*. Here, we examine the capacity of this targeted vector to induce immune responses to the tumor antigen CEA in a stringent *in vivo* canine model. CD40-targeted Ad5 transduced canine DCs via the CD40-CD40L pathway *in vitro*, and following vaccination of healthy dogs, CD40-targeted Ad5 induced strong anti-CEA cellular and humoral responses. These data validate the canine model for future translational studies and suggest targeting of Ad5 vectors to CD40 for *in vivo* delivery of tumor antigens to DCs is a feasible approach for successful cancer therapy.

1. Introduction

Many immunological features of cancers that allow evasion of immune surveillance and destruction have been revealed, enabling the development of new and more effective immunotherapeutic strategies. Immune evasion is now recognized to be due primarily to a breakdown in the normal route of tumor antigen presentation to T cells [1]. In order to mount an immune response against a tumor, antigen presenting cells (APCs) monitoring peripheral tissues must present tumor-associated antigens (TAA) to T cells. In a fully functional immune system, APCs capture and present TAA to CD8+ T cells (lymphocytes) (CTL) and CD4+ helper T (Th) cells in lymph nodes (LN), leading to the expansion and activation of antigen-specific effector T cells. Once activated, CTLs recognize tumor cells expressing the presented TAA. The identification of a variety of cancer-specific TAA has provided more options for immunotherapy; however, TAA are often self-antigens to which a considerable immunological tolerance is maintained, especially depending on the route of T cell presentation [2]. Therefore, strategies for overcoming tolerance and generating effective immune responses against TAA are being developed based on harnessing the immunostimulatory activity of APCs.

Delivering TAA specifically to dendritic cells (DCs) with an antigen-delivery system offers tremendous potential for the development of new cancer vaccines [3]. Supporting this, pre-clinical and clinical trials have focused on adoptive transfer of TAA-exposed DCs. These approaches involve isolating DCs from the blood of patients, exposing the DCs to TAA and other maturation stimuli in

* Corresponding author at: University of Alabama at Birmingham, 901 19th Street South BMR2-508, Birmingham, AL 35294-2172, United States. Tel.: +1 205 934 8627; fax: +1 205 975 7476.
E-mail address: curiel@uab.edu (D.T. Curiel).

0264-410X/$ – see front matter © 2009 Elsevier Ltd. All rights reserved.
doi:10.1016/j.vaccine.2009.09.055

culture, and finally, re-injecting them into the patient. Although encouraging results have been reported, there are substantial medical, economic, and logistic complexities to this approach. In addition, while pre-clinical trials in mice demonstrated highly promising immune responses, including tumor regression and remission, clinical trials in humans resulted in far fewer cases of tumor stability or regression, suggesting these vaccines are not yet optimal [4–8]. Possibly underlying these results, recent evidence indicates that DCs matured *ex vivo* do not accurately mimic DCs matured *in vivo*, precluding optimal immune system stimulation [9]. Thus, a strategy to facilitate DC transduction to mediate TAA delivery *in vivo* that is universally efficacious, regardless of haplotype, is required.

In regard to DC transduction efficiency, gene transfer and immune stimulation, viral transduction methods have been found to be superior to non-viral methods [10–12]. In addition to high gene transfer efficiency, transduction of DCs with adenovirus serotype 5 (Ad5)-based vectors offers many benefits over other viral vectors. Ad5-mediated transduction does not require cell proliferation and poses a low risk for insertional mutagenesis [13–16]. Furthermore, non-replicating Ads provide the additional benefit of delivering TAA for only a finite amount of time, thus minimizing the chances of inducing hyporesponsiveness to chronic antigen presentation. Despite these advantages, DCs are relatively refractory to Ad5 transduction due to limited cell surface expression of the primary Ad5 receptor, coxsackie virus and adenovirus receptor (CAR) [17]. Thus, efficient Ad5-mediated gene transfer to DCs requires high multiplicities of infection (MOI). To overcome this, our lab has re-targeted Ad5 to CD40 expressed on cell surfaces, achieving efficient and specific DC transduction and antigen-specific immune responses using low doses of Ad5 administered subcutaneously, a site enriched for DCs [17–25]. In addition to providing a means for efficient DC transduction, CD40 ligation and activation induces migration of mature DCs to the T cell populated areas of the draining lymph node, thus CD40-targeted vectors are likely to provide additional immunotherapeutic benefits.

In the experiments presented here, the transduction potential of CD40-targeted Ad5 was determined in canine DCs, and the immunostimulatory capacity of this targeting strategy was evaluated in dogs, the most relevant translational animal model available for evaluating many therapeutic modalities designed to combat human diseases. Of particular relevance to our studies, dogs are naturally susceptible to several cancers which mimic the onset, progression and symptoms of the corresponding human cancers, allowing therapeutic evaluation with increased clinical relevance [26–29]. Indeed, many advances in human cancer therapies have been made or improved through studies in canine patients, including the first evaluations of cancer vaccines, and the analysis of cytokine and chemotherapeutic regimens for pulmonary metastases [26]. In addition, canine models provide dosing and vector production challenges similar to those encountered in human clinical trials [26,30,31].

The data presented from this pilot study in healthy dogs validate the utility of the canine model for our translational studies, and suggest that specific targeting of Ad5 vectors to DCs for *in vivo* delivery of genes encoding TAA may provide an enhanced immune response to disease-related antigens.

2. Materials and methods

2.1. Cell lines

The human embryonic kidney cell line 293 was purchased from Microbix (Toronto, Ontario, Canada). The 293F28 and 293/hCD40 cell lines are derivatives of 293 cells which express either Ad5 wild-type fiber (for mosaic virus propagation as described below) or human CD40 as previously described [21]. The 293/cCD40 cell line is a derivative of the 293 cell line which expresses canine CD40, and was generated by transfection of 293 cells with the plasmid pcDNA3.1canineCD40, and subsequent selection with 1000 μg/ml of Geneticin (G418). A cell clone derived from this population that expressed high levels of canine CD40 was identified by RT-PCR. All 293 and 293-derived cell lines were propagated in a 50:50 mixture of Dulbecco's modified Eagle's medium and Ham's F-12 medium (DMEM/F-12) supplemented with 10% (v/v) fetal calf serum (FCS), L-glutamine (2 mM), penicillin (100 units/ml) and streptomycin (100 μg/ml). FCS was purchased from Gibco-BRL (Grand Island, NY) and media and supplements were from Mediatech (Herndon, VA). RT-PCR analysis of cell lines revealed 4.47×10^7 copies/μg of human CD40 mRNA in 293/hCD40 compared to 5.6×10^{-2} copies/μg in control 293 cells, and 6.44×10^3 copies/μg of canine CD40 mRNA in 293/cCD40 cells. 293F28 cells were maintained with 100 μg/ml Zeocin (Invitrogen), and 293/hCD40 and 293/cCD40 cells were maintained with 100 μg/ml G418. All cell lines were cultured at 37 °C in 5% CO_2.

2.2. Gene therapy vectors

Ad5.FFhCD40L vectors expressing artificial fiber proteins containing FF-CD40L and encoding either luciferase, CEA or GFP/CEA were constructed as previously described [20,21]. Ad5 vectors expressing the native fiber protein and encoding either luciferase, GFP/luciferase or CEA were employed as controls [20,32,33]. Briefly, Ad5 vectors encoding the native fiber protein were generated by transfection of 293 cells with Pac I-digested Ad rescue vectors. Vectors with FF-CD40L were generated by transfection of 293F28 cells with Pac I-digested Ad rescue vectors. 293F28 cells stably express the native Ad5 fiber, thus viruses rescued at this point were mosaic in the sense that the Ad5 virions randomly incorporated a mixture of native fibers and FF-CD40L chimeras. After additional rounds of amplification on 293F28 cells, the viruses were amplified in 293 cells, which do not express native Ad5 fiber, to obtain virus particles containing only FF-CD40L [21].

All Ad5 vectors were isolated from infected cells and purified by equilibrium centrifugation in CsCl gradients according to a standard protocol [34]. The protein concentrations in the viral preparations were determined using the DC protein assay (BioRad, Hercules, CA) with purified bovine serum albumin (BSA) as a standard. The virus titers were calculated using the formula: 1 μg of protein = 4×10^9 viral particles (vp).

2.3. Preparation of canine peripheral blood mononuclear cell populations

Whole blood (40–60 ml) was collected from normal outbred dogs in EDTA tubes (Becton, Dickinson), gently and thoroughly mixed and centrifuged 30 min at $1000 \times g$ at RT. The buffy coat containing the peripheral blood mononuclear cell (PBMC) population was extracted with a pipette in 1–2 ml and diluted with 8 ml HBS (HEPES-buffered saline, no Mg/Ca, Gibco/BRL). The cell suspension was layered over 5 ml Histopaque 1077 (Sigma–Aldrich) and centrifuged at $1000 \times g$ at RT for 30 min. The band containing the PBMC population was extracted in 1–2 ml into a new sterile tube and diluted with 2 ml HBS, mixed, and centrifuged once more. The supernatant was removed and the cells gently resuspend in 5 ml HBS. The cells were centrifuged once more and resuspended in 4 ml flow wash buffer (FWB–HBS containing 10% fetal bovine serum) and incubated at RT at least 40 min to allow blocking of nonspecific sites.

2.4. Flow cytometry and fluorescent activated cell sorting for canine dendritic cells

Antibodies were obtained that recognize canine CD11c (monoclonal mouse anti-dog CD11c, Serotec) and human CD40 (monoclonal mouse clone B-B20, prelabeled with Zenon reagent PE/Alexa Fluor 610, Invitrogen). The PBMC suspension was centrifuged at 200 × *g* at RT for 10 min, the supernatant removed, and the cells resuspended in 1 ml FWB. Primary antibodies (100 μl each) were then added, gently mixed, and incubated for 60 min at RT in the dark. Then, 2 ml HBS was added and the cell suspension centrifuged at 200 × *g* for 10 min. The supernatant was aspirated and the cells were washed two additional times in 2 ml HBS, finally resuspending them in 1 ml FWB. Each cell suspension was filtered to 50 μm in a sterile CellTrics disposable filter (Partec, Germany).

Flow cytometry assays and fluorescent activated cell sorting (FACs) were performed on a MoFlo flow cytometer and cell sorter (Beckman Coulter). The CD11c expression profiles were determined using Summit 4.0 software (Beckman Coulter). The entire cell suspension was sorted for each experiment and sorted cells (CD11c+ and CD11c−) sterilely collected into tubes containing 1 ml of FBS. Both samples and sorted populations of cells were maintained at RT during the entire process.

To ensure recovery of exposed CD40 on the cell surface, cells were allowed to recover for 4 h prior to transduction with Ad vectors. Following transduction, cells were collected by centrifugation, and brought into culture in RPMI-1640 (Gibco/BRL) containing 10% FBS, penicillin/streptomycin/fungizone (Gibco/BRL) and 25% lymphocyte conditioned media (CM). CM was obtained from cultures of freshly prepared canine lymphocytes which had been stimulated for 24–48 h with phytohemagglutinin (PHA, 10 μg/ml, Sigma–Aldrich) [35,36].

2.5. Recombinant protein purification and western blot analysis

The 6-HIS-tagged soluble human CD40L protein and its derivatives were expressed in *Escherichia coli* BL21(DE3)(pLysS) as previously described [21]. The concentrations of the proteins in purified preparations and in cell lysate were determined using the BioRad DC protein assay.

2.6. Gene transfer experiments

293, 293/hCD40 and 293/cCD40 cell lines and canine DCs were plated in 24-well plates at 1×10^5 cells/well. Prior to transduction, cells were washed with serum-free growth medium and incubated on ice with 0.2 ml of either medium or medium containing a blocking agent. In the latter instance, recombinant Ad5 fiber knob [37] or soluble hCD40L proteins were added to the medium at concentrations of 100 μg/ml for 1 h on ice. Cells were transduced at a multiplicity of infection (MOI) of 10, 100 or 1000 vp per cell with Ad5 vectors in medium containing 2% FCS. After incubation on ice for 1 h, the medium containing the virus and the inhibitor was removed, and cells were washed with medium containing 10% FCS. Fresh medium was added, and incubation was continued at 37 °C for 22 h to allow reporter gene expression. Cells were then washed with PBS and lysed in Luciferase Reporter Lysis Buffer (Promega). The luciferase activity in the cell lysates was measured according to the manufacturer's protocol. Each data point was assessed in triplicate and calculated as the mean of three determinations. In instances where transduction was performed without the addition of a blocking agent, the virus was added to the cells in 0.4 ml aliquots of medium containing 2% FCS.

All incubation and washing steps in gene transfer experiments involving DCs were performed in cell suspensions since these cells are only loosely adherent. To minimize variation in the data, which could result from the loss of cells during the washing steps, the luciferase activity measured in the cell lysates was normalized to the protein concentration of resulting cell lysates.

2.7. In vivo canine vaccinations

All experiments were conducted under the oversight of the Auburn University IACUC committee in AAALAC approved animal and clinical care facilities. Outbred beagle dogs from two litters were used for vaccination. The dogs were 10 and 15 weeks of age at the start of the experiment and weighed approximately 10–15 kg each. Additional adult beagle and beagle-corgi crosses were used to provide blood for isolation of PBMCs. 1×10^9 vp of Ad5CEA.FF/hCD40L (five dogs) or control Ad5CEA (five dogs) vectors were delivered in 0.5 ml sterile phosphate-buffered saline (PBS) to each dog. Intradermal (i.d.) injections were performed in the right lower abdomen using a 25 gauge needle. The dogs were re-injected with the same dose of each Ad5 vector and by the same route as their original injection on weeks 4, 8 and 12. Peripheral blood was collected each week and used for ELISA detection of anti-CEA antibodies. At week 14, lymphocytes were purified from collected peripheral blood for lymphoproliferation assays.

2.8. Lymphoproliferation assays

PBMCs were obtained by density gradient centrifugation using lymphocyte separation media (Cellgro, Mediatech, Inc, Herndon, VA) and were resuspended in complete medium consisting of RPMI 1640 supplemented with 10% fetal bovine serum, 2 mM L-glutamine, 50 μM 2-mercaptoethanol, and antibiotics. Cells were added at 1×10^5 cells per well in round bottom 96-well plates. Stimulated cells were incubated in triplicate wells with recombinant human CEA protein (Vitro Diagnostics, Inc. Aurora, CO) over a range of concentrations (1–30 μg/ml). Additionally, BSA (30 μg/ml) or ovalbumin (OVA) (25 μg/ml) wells were included as negative control antigens and Con-A wells (0.5 μg/ml) were included as positive control mitogens. Control cells were cultured in complete medium alone. All cells were incubated at 37 °C in a humidified atmosphere of 5% CO_2 in air for two days, followed by an overnight pulse with 1 μCi/well of tritiated thymidine diluted at 50 μCi/ml. Cells were harvested and incorporated radioactivity was quantified using a solid-phase beta scintillation counter (Matrix 9600; Packard Instrument Co., Downers Grove, IL). The Stimulation Index (S.I.) was calculated as the mean counts per million (cpm) of the stimulated cells divided by the mean cpm of the control (OVA-stimulated) cells. A positive response was defined as a post-vaccination S.I. >3.0. The assay was performed in triplicate for each sample and results are presented as means.

2.9. ELISA for detection of anti-CEA antibodies

For CEA antibody detection, 96-well EIA plates (Costar 3590) were coated with recombinant CEA protein (Vitro Diagnostics, Inc. Aurora, CO) at 100 ng/well in borate saline (BS) buffer, pH 8.4, for 4 h at RT, and then blocked with borate saline plus 1% (w/v) bovine serum albumin (BS-BSA). Serial three-fold dilutions of dog serum in BS-BSA (1:50–1:109,350) were added to the wells and incubated overnight at 4 °C. Plates were washed with PBS containing 0.05% (v/v) Tween-20 and incubated with AP conjugated rabbit anti-dog (IgG H+L) antibodies (Jackson Immunoresearch Laboratories, Inc. West Grove, PA) diluted 1:2000 in BS-BSA for 4 h at RT. After washing, AP substrate (*p*-nitrophenyl phosphate, Sigma St. Louis, MO) in diethanolamine buffer, pH 9.0, was added and incubated for 20 min at RT. Absorbance was measured at 405 nm on

a Multiskan Ascent microplate reader using Ascent software (Labsystems OY, Helsinki, Finland). Absorbance on CEA coated plates was corrected for absorbance on parallel plates coated with ovalbumin (Sigma–Aldrich Chemical Co., St. Louis, MO). COL-1 mouse monoclonal antibody to CEA (NeoMarkers, Fremont, CA) followed with AP conjugated goat anti-mouse IgG (Southern Biotechnology, Birmingham, AL) was used as a positive control. For detection of IgG isotypes goat anti-dog IgG1 and sheep anti-dog IgG2 antibodies conjugated to horseradish peroxidase (Bethyl Laboratories Inc., Montgomery, TX) were applied to the wells at a dilution of 1:10,000. After incubation and wash 3,3′, 5′5 tetramethyl benzidine substrate (Sigma) was applied for colorimetric development. The reaction was stopped by adding 0.5 M H_2SO_4 and absorbance was read at 450 nm. Statistical analysis was performed by using two-tailed Student's *t*-test and values are presented as mean ± standard error of the mean.

3. Results

3.1. Generation of CD40-targeted Ad5

Human, rhesus and murine DCs have been successfully transduced with CD40-targeted Ad5 *in vitro*, resulting in selective transduction and simultaneous activation of DCs, indicating CD40 is an effective target in many species [17–24,38,39]. To establish the principle that CD40-targeted Ad5 can also mediate gene transfer to canine DCs, we employed a genetically engineered Ad5 vector encoding firefly luciferase, designated Ad5Luc.FF/hCD40L (Fig. 1) [19,21]. This vector was previously constructed so that the shaft and knob domains of the native fiber protein are replaced by phage T4 fibritin (as a trimerization motif) genetically fused to the TNF-Like (TNF-L) ectodomain of human CD40L (Fig. 1A). The presence of the phage T4 fibritin structure allows the TNF-L ectodomain of CD40L to retain its functional tertiary structure, required for activation of CD40 [21]. Human and canine CD40 are 83% similar, and amino acids predicted to be involved in CD40-CD40L binding are conserved [40,41], suggesting an Ad5 vector expressing human CD40L may interact effectively to allow transduction of CD40-expressing canine cells.

3.2. Gene transfer analysis in 293 cells expressing CD40

To confirm that the human CD40L ectodomain of Ad5Luc.FF/hCD40L mediates vector targeting to canine CD40, luciferase transgene expression was analyzed as a measure of vector transduction potential in 293 cells and cell lines stably

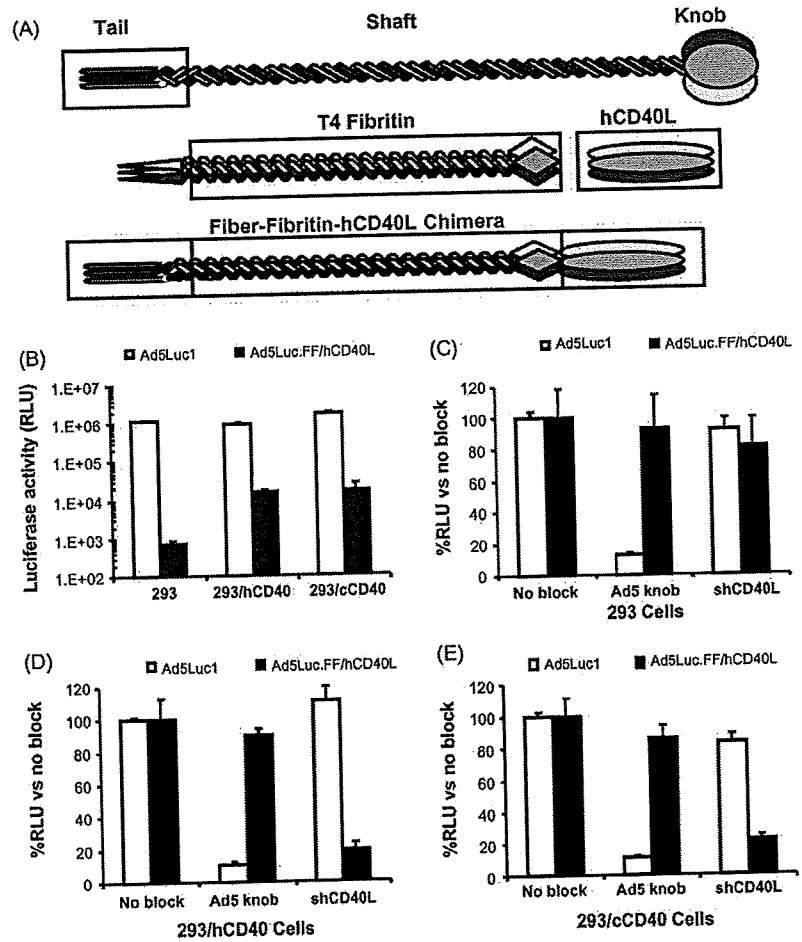

Fig. 1. Efficiency of gene transfer and receptor specificity of CD40-targeted Ad5. (A) Schematic diagram of CD40-targeted Ad5. The shaft and knob domains of native Ad5 fiber were replaced by phage T4 fibritin genetically fused to the TNF-L ectodomain of human CD40L. (B) 293, 293/hCD40 and 293/cCD40 cells were transduced with untargeted Ad5Luc1 (white bars) or CD40-targeted Ad5Luc.FF/hCD40L (black bars) at an MOI of 10 vp/cell. To determine receptor specificity, 293 (C), 293/hCD40 (D) and 293/cCD40 (E) cells were transduced with untargeted Ad5Luc1 (white bars) or CD40-targeted Ad5Luc.FF/hCD40L (black bars) at an MOI of 10 vp/cell. Prior to infection with virus, cells were incubated with recombinant Ad5 fiber knob or shCD40L to block transduction through CAR or CD40, respectively. 24 h after transduction, luciferase activity was determined as a measure of Ad5-mediated gene transfer. Luciferase activity is expressed as relative light units. Luciferase activity detected in the presence of blocking agents is normalized against luciferase activity in absence of blocking agents. Mean ± SD are shown from three replicates performed simultaneously.

expressing CD40. 293 cells, which do not express endogenous CD40, or 293 cells stably transfected with either human CD40 (293/hCD40) or canine CD40 (293/cCD40) were incubated with either untargeted Ad5Luc1 or CD40-targeted Ad5Luc.FF/hCD40L (10 vp/cell) (Fig. 1B). All 293 cell lines, which express the Ad5 receptor, CAR, were efficiently transduced by untargeted Ad5Luc1. In contrast, wild-type 293 cells incubated with Ad5Luc.FF/hCD40L expressed very low levels of luciferase, indicating this CD40-targeted vector does not transduce cells efficiently through CAR. However, Ad5Luc.FF/hCD40L-mediated luciferase expression in both 293/hCD40 and 293/cCD40 cells (Fig. 1B), suggesting Ad5Luc.FF/hCD40L capably transduces cells expressing either human or canine CD40.

3.3. Validation of CD40-mediated transduction

To further investigate the targeting specificity of Ad5Luc.FF/hCD40L, viral transduction was performed in the presence of specific blocking agents. Prior to transduction, 293, 293/hCD40 and 293/cCD40 cells were incubated with either soluble recombinant Ad5 fiber knob or soluble human CD40L (shCD40L) to block CAR or CD40, respectively, on the cell surface. Luciferase expression under these blocking conditions was compared to luciferase expression without blocking (normalized for each vector to 100%). As shown in Fig. 1(C–E), transduction of all 293 cell lines by Ad5Luc1 was inhibited by soluble knob (87% block in 293 cells, and 90% block in 293/hCD40 and 293/cCD40), indicating transduction by untargeted Ad5 requires CAR, as expected. The very low level of luciferase expression in 293 cells incubated with Ad5Luc.FF/hCD40L was not affected by soluble Ad5 knob (Fig. 1C). The high luciferase expression levels in 293/hCD40 and 293/cCD40 cells transduced by Ad5Luc.FF/hCD40L were not affected when CAR was blocked with soluble Ad5 knob (Fig. 1D and E), further demonstrating that Ad5Luc.FF/hCD40L does not require CAR for transduction of CD40-expressing cells. In contrast, pre-incubation with shCD40L decreased luciferase expression levels by 81% in 293/hCD40 cells, and by 78% in 293/cCD40 cells (Fig. 1D and E), but did not affect luciferase expression levels following Ad5Luc1 transduction in 293 cells (Fig. 1C). These results demonstrate that transduction by Ad5Luc.FF/hCD40L specifically requires cellular expression of CD40.

3.4. Targeted gene transfer to canine cells

To determine if CD40-targeted Ad5 also transduces canine DCs, as observed with DCs from other species, transduction experiments were conducted with canine DCs cultured from isolated PBMCs. Flow cytometry with anti-CD40 and -CD11c antibodies indicated CD40 expression on 43.5% of CD11c+ PBMCs (DCs), while only 1.7% of CD11c– cells were CD40+ (Fig. 2A). Based on CD40 expression, DCs were sorted into two groups: CD11c+/CD40– and CD11c+/CD40+. Cells from each group were incubated with either Ad5Luc1 or Ad5Luc.FF/hCD40L for analysis of transduction efficiency as measured by luciferase expression levels. As observed previously with human DCs [17], canine CD11c+/CD40+ DCs were refractory to transduction by untargeted Ad5, even at a very high vector concentration of 1000 vp/cell (Fig. 2B). In contrast, luciferase transgene expression was 15-fold higher in

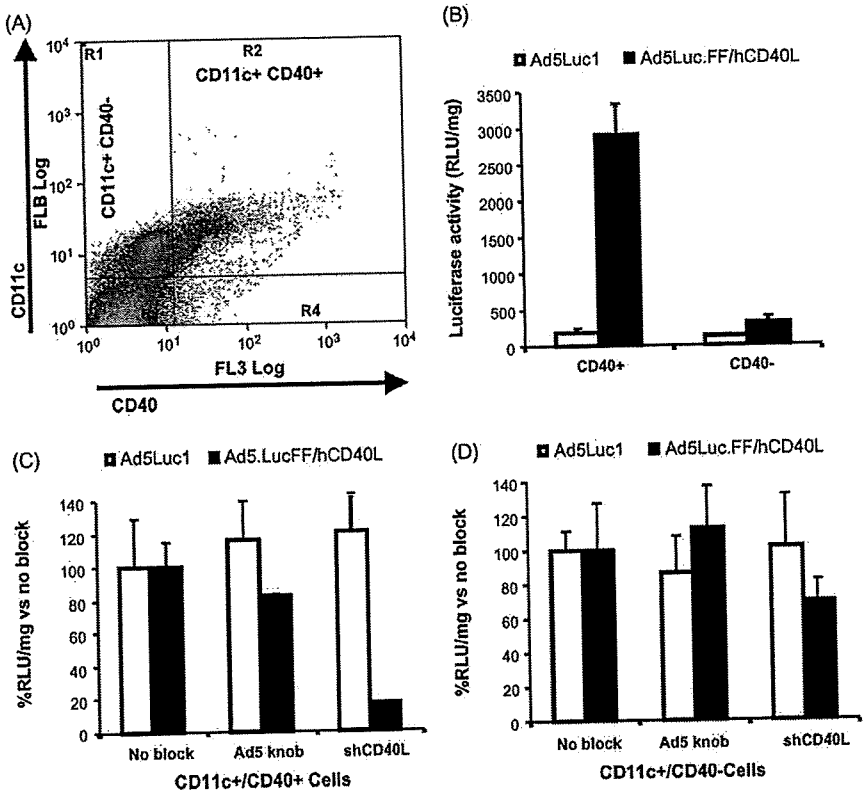

Fig. 2. Receptor specificity of cell transduction and efficiency of gene transfer mediated by CD40-targeted Ad5 in canine DCs. (A) Anti-CD40 antibodies detected expression of CD40 on 43.5% CD11c+ cells, and cells were sorted cells based on CD40 expression levels. (B) CD11c+/CD40+ and CD11c+/CD40– cells were transduced with untargeted Ad5Luc1 (white bars) or CD40-targeted Ad5Luc.FF/hCD40L (black bars) at an MOI of 1000 vp/cell to determine the receptor specificity of vector transduction. (C) CD11c+/CD40– and (D) CD11c+/CD40+ canine cells were transduced with untargeted Ad5Luc1 (white bars) or CD40-targeted Ad5Luc.FF/hCD40L (black bars) at an MOI of 1000 vp/cell in the presence of recombinant Ad5 fiber knob or soluble human CD40L to further confirm the receptor specificity of vector transduction. Luciferase activity detected in the presence of blocking agents is normalized against luciferase activity in absence of blocking agents. Mean ± SD are shown from three replicates performed simultaneously.

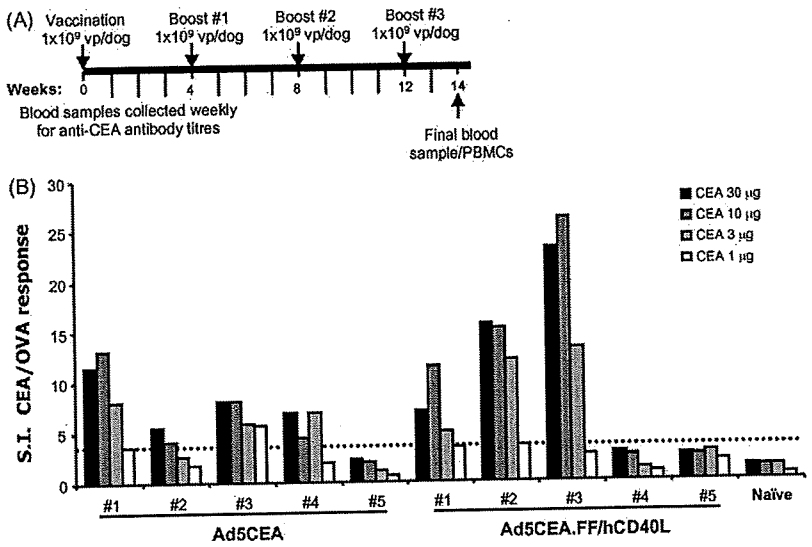

Fig. 3. Antigen-specific lymphocyte responses in healthy dogs vaccinated with CD40-targeted Ad5. (A) On day 0, five dogs were vaccinated i.d. with Ad5CEA (1×10^9 vp/dog) and five dogs were vaccinated with Ad5CEA.FF/hCD40L (1×10^9 vp/dog). At 4, 8 and 12 weeks post-vaccination, each dog received a booster injection (1×10^9 vp/dog) of the same vector. Blood was drawn at 14 weeks post-vaccination for lymphoproliferation assays. (B) Harvested PBMCs were stimulated for two days with recombinant human CEA at a range of concentrations (1–30 µg) or ovalbumin (25 µg) followed by an overnight pulse with tritiated thymidine. Cells were harvested and incorporated radioactivity was quantified. The S.I. was calculated as the mean cpm of the stimulated cells divided by the mean cpm of the ovalbumin-stimulated cells. A positive response was defined as a post-vaccination S.I. >3.0 (denoted by dotted line).

CD11c+/CD40+ DCs incubated with Ad5Luc.FF/hCD40L. Transgene expression was only slightly increased in CD11c+/CD40– DCs following incubation with Ad5Luc.FF/hCD40L, suggesting this vector specifically transduces cells via CD40. This minimal increase in Ad5Luc.FF/hCD40L-mediated gene transfer in CD11c+/CD40– DCs may be due to low-level expression of CD40 in this CD11c+ subset that could not be detected by flow analysis. Supporting this, luciferase expression was 84% lower in CD11c+/CD40+ cells pre-incubated with shCD40L and transduced with Ad5Luc.FF/hCD40L, but only 30% lower in CD11c+/CD40– cells pre-incubated with shCD40L (Fig. 2C and D). Furthermore, when transductions were performed with vectors encoding GFP, GFP expression was detected only in CD11c+/CD40+ cells incubated with the CD40-targeted vector. GFP expression was not detected in CD11c+/CD40– cells incubated with CD40-targeted vector or in either DC subset incubated with untargeted vector (Supplementary Fig. 1). These results again confirm the specificity of CD40-mediated transduction by this CD40-targeted Ad5 vector. Thus, the efficient and specific delivery of transgenes to canine DCs by Ad5Luc.FF/hCD40L *in vitro* validates the examination of this vector for *in vivo* delivery of transgenes to CD40-expressing cells, particularly DCs.

3.5. *Antigen-specific immune responses following vaccination in healthy dogs*

The ultimate goal is the development of a vaccine that can deliver tumor-specific transgenes to DCs *in vivo* in order to generate a TAA-specific immune response. Therefore, it was critical to investigate the capacity of untargeted versus CD40-targeted Ad5 vectors to induce TAA-specific immune responses. We have previously demonstrated an enhanced immune response in mice following injection of CD40-targeted Ad5 by various routes [25]. To determine if similar immune responses are detected in dogs, we performed a pilot experiment with healthy dogs injected with Ad5 vectors engineered to express human carcinoembryonic antigen (CEA) as a model tumor antigen (Ad5CEA and Ad5CEA.FF/hCD40L). CEA orthologues have been identified in dogs; however xenoantigens are more likely to overcome immunotolerance and induce a more robust antigen-specific immune response [42–45]. Five dogs received i.d. injections of Ad5CEA (1×10^9 vp/injection) and five dogs received injections of Ad5CEA.FF/hCD40L (1×10^9 vp/injection) according to the schedule outlined in Fig. 3A. One dog served as a negative control, receiving no injections. At week 14, PBMCs were harvested and lymphocyte proliferation was quantified as a measure of TAA-specific T cell activation. An S.I. of greater than 3.0 was considered positive. A positive lymphoproliferative response was observed in three of five dogs immunized with Ad5CEA.FF/hCD40L and in four of five dogs immunized with Ad5CEA, although the average S.I. tended to be greater in responding animals immunized with Ad5CEA.FF/hCD40L (Fig. 3B). These results suggest that while vaccination with either untargeted or CD40-targeted Ad5 induces an antigen-specific T cell response, this response may be magnified in individuals responding to the CD40-targeted vector.

To analyze antigen-specific humoral immune responses, CEA-specific IgG serum concentrations were quantified. A strong anti-CEA humoral immune response was induced in both groups of dogs by 14 days post-immunization, though the antibody titer of dogs immunized with untargeted Ad5CEA was significantly higher as measured on days 21, 35 and 42 (Fig. 4A). We further examined the isotype of the antibody response on day 35, the day with the most significant difference in antibody responses between the groups. The concentration of IgG1 was significantly lower in dogs immunized with Ad5CEA.FF/hCD40L (Fig. 4B and C), resulting in a higher ratio of IgG2 to IgG1 (Fig. 4D).

4. Discussion

DC-based vaccination can overcome tumor-associated suppression of immune responses, although the full potential of this strategy has yet to be realized in the context of a reliable cancer therapy [4–8]. In order to overcome the potential limitations associated with autologous DCs transduced and matured *ex vivo*, our lab has investigated methods to directly transduce and activate DCs *in vivo* in a an animal model highly likely to provide clinically relevant information.

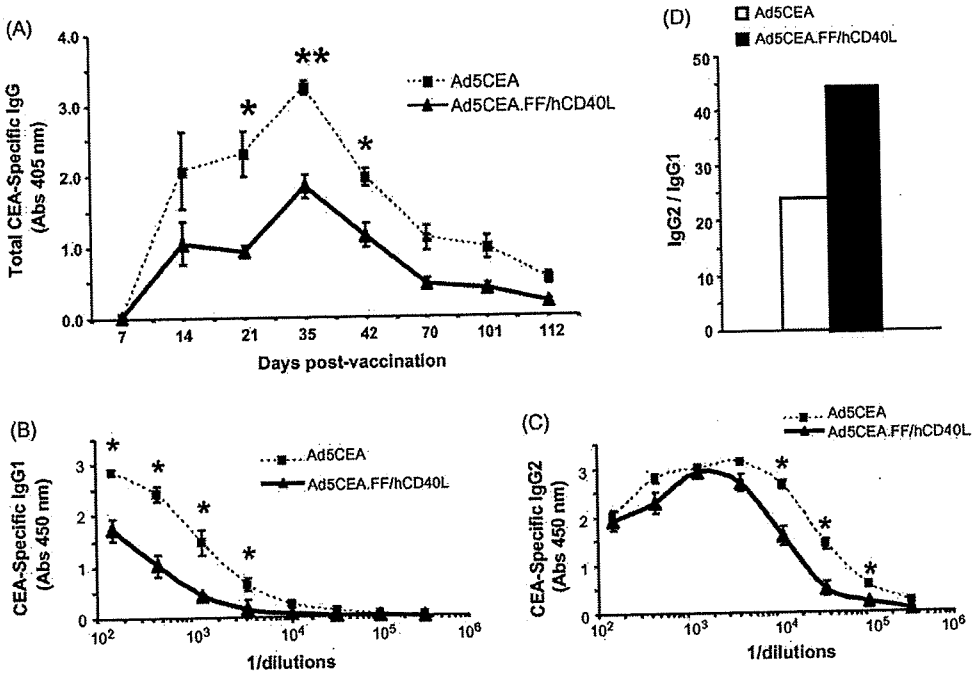

Fig. 4. Antigen-specific humoral responses in healthy dogs vaccinated with CD40-targeted Ad5. (A) Serum was drawn weekly from each dog following vaccination with Ad5CEA (squares) or Ad5CEA.FF/hCD40L (triangles). ELISAs were performed to detect human CEA-specific canine IgGs. Serum from each time point was incubated with recombinant human CEA, and detected with anti-dog IgG secondary antibody to determine total IgG concentrations. (B) IgG1 and (C) IgG2 isotypes were detected with goat anti-dog IgG1 and sheep anti-dog IgG2 antibodies, respectively. (A, B and C) Absorbance was read at 450 nm. Statistical analysis for was performed by using two-tailed Student's *t*-test and values are presented as mean ± SE. $^{*}p < 0.05$; $^{**}p < 0.0001$. (D) Average ratio of IgG2:IgG1 following vaccination with Ad5CEA (white) or Ad5CEA.FF/hCD40L (black).

Several strategies to accomplish *in vivo* delivery of immunotherapeutic antigens to DCs have now been reported, including the use of free antigen, protein fusions and viral gene therapy [46–51]. However, complete success depends on overcoming biological delivery challenges. In this regard, Arthur et al. previously found that Ad5 vectors are superior to other non-viral methods for delivering antigens to DCs *in vitro* [10], and other groups have since demonstrated highly efficient Ad5-mediated gene transfer to DCs *ex vivo*, using high concentrations of Ad5 [52,53]. Additionally, Ad5 capsid protein is a potent adjuvant that enhances CTL response [54]. Therefore, TAA transfer by Ad5 vectors is likely to enhance production of tumor cell-specific CTL [55]. Thus, an Ad5 vector re-targeted to bind a specific protein expressed on the surface of DCs seems likely to provide an enhanced *in vivo* immunotherapeutic strategy.

In addition to targeting DCs, proper activation and maturation of DCs is crucial for stimulating an antigen-specific immune response. It is now obvious that the collective term "DC" actually refers to a heterogeneous population of cells, derived from different lineages, in different maturation states, and likely displaying distinct functional features [8]. In general, antigen presentation by mature DCs leads to an antigen-specific immune response, while antigen presentation by immature DCs has been implicated in the induction of immune tolerance through activation of regulatory T cells [56]. CD40 is an attractive candidate for targeting DCs as it is expressed on the cell surface of DCs, and, while it is also expressed on endothelial cells and other immune cells, CD40 expression is far less ubiquitous than CAR expression. Additionally, localized dermal injection of CD40-targeted virus delivers virus to a location that is rich in CD40-positive DCs and lacks substantial numbers of other CD40-expressing cells, such as B cells. Binding of CD40L to CD40 induces DC maturation, enabling these cells to migrate to draining lymph nodes and activate antigen-specific T cells. This complete activation of DCs is critical for tumor rejection *in vivo* [57].

Results from the analysis of our *in vitro* gene transfer in model cell lines and canine DCs demonstrates CD40-targeting dramatically enhances Ad5-mediated transgene expression in cells expressing CD40, and in DCs in particular. Furthermore, CD40-targeted Ad5 requires cell expression of CD40 for transduction, and is incapable of transducing cells through CAR. This specificity will likely allow *in vivo* transduction of DCs with a much lower vector dose than is required for untargeted Ad5 transduction. Studies are currently underway to confirm the *in vivo* cell specificity of CD40-targeting.

In order to obtain clinically relevant information regarding the immune response generated *in vivo* following vaccination with CD40-targeted Ad5, we immunized healthy dogs with CD40-targeted or untargeted Ad5 encoding human CEA as a model tumor antigen. A key issue in the successful development of effective cancer immunotherapies is the design of vaccines that can overcome immune tolerance and induce a T cell response to autologous TAA, which are also expressed by normal cells. In this regard, experiments in mouse models suggested that vaccination with xenogeneic TAAs (xenoantigens) encoding slight differences in sequence overcome immune tolerance by improving MHC I and II epitope presentation, evoking tumor immunity [42–45]. Thus, using Ad5 vectors encoding human CEA allowed us to more thoroughly investigate the potential of eliciting TAA-specific immune responses in dogs via a CD40-targeted Ad5 vector.

Antigen-specific T cell responses were generated in dogs receiving either the CD40-targeted vector or the untargeted vector. Interestingly, the extent of lymphoproliferation appeared to be enhanced in responders immunized with CD40-targeted Ad5 as compared to untargeted Ad5, though these responses will need to be investigated with a larger number of dogs in order to thoroughly evaluate statistical significance. Further, as observed with previous studies in mice [25], an antigen-specific humoral response was also observed following vaccination with either CD40-targeted

or untargeted vectors in all dogs. However, a clear difference in the quality of the response was detected in the ratio of IgG1 to IgG2 isotypes generated by the two vectors. Though the relationship between Th type responses and IgG subclass has not been completely characterized in dogs [58], previous reports suggest that increased IgG2 production correlates with a Th1 type immune response that is characterized by a cytokine profile similar to that in humans [59–62]. Also similar to human patients, Th1 inducing cells, as determined by cytokine production, are diminished in dogs with metastatic cancers [63]. Suppression of DC-activated Th1 immunity has been implicated in the progression of cancers such as melanoma, thus an enhanced antigen-specific Th1 cellular immune response is likely to result in a more effective anti-tumor response. Future studies measuring cytokine release by T cells will be required for complete evaluation of the immune response generated, however.

In summary, these results from a pilot vaccination study in dogs confirm in a clinically relevant animal model that re-targeting Ad5 to bind CD40 circumvents the requirement for CAR expression, allowing efficient transgene expression in DCs *in vitro*, and subsequent antigen-specific immune responses *in vivo*. CD40-targeted Ad5 may in turn provide more effective cancer therapies. Most importantly, immune responses in these dogs are comparable to expected responses in humans, and establish that dogs provide a reliable intermediate model system for investigating potential immunotherapies for cancers such as osteosarcoma, lymphoma, breast cancer and melanoma. Thus, these experiments have provided the critical groundwork necessary to allow further evaluation of targeted immunotherapies in canine cancer patients in order to provide information for development of successful translational therapies.

Acknowledgements

The authors thank A. Church Bird for valuable consultations on FACs and flow cytometry, Dr. Sandra Ewald for critical advice for optimizing DC culture conditions, and Dr. Maaike Everts for critical reading of the manuscript. This work was supported by: 1R01 CA113454 to BFS, NIAMS P30-AR050948 to LT and NIH training grants T32 CA075930-09 and T32 AR053458-01 to ET.

Appendix A. Supplementary data

Supplementary data associated with this article can be found, in the online version, at doi:10.1016/j.vaccine.2009.09.055.

References

[1] Chen L. Immunological ignorance of silent antigens as an explanation of tumor evasion. Immunol Today 1998;19(1):27–30.
[2] Geijtenbeek TB, van Vliet SJ, Engering A, t Hart BA, van Kooyk Y. Self- and nonself-recognition by C-type lectins on dendritic cells. Annu Rev Immunol 2004;22:33–54.
[3] O'Hagan DT, Valiante NM. Recent advances in the discovery and delivery of vaccine adjuvants. Nat Rev Drug Discov 2003;2(9):727–35.
[4] Mosca PJ, Lyerly HK, Clay TM, Morse MA, Lyerly HK. Dendritic cell vaccines. Front Biosci 2007;12:4050–60.
[5] Cerundolo V, Hermans IF, Salio M. Dendritic cells: a journey from laboratory to clinic. Nat Immunol 2004;5(1):7–10.
[6] den Brok MH, Nierkens S, Figdor CG, Ruers TJ, Adema GJ. Dendritic cells: tools and targets for antitumor vaccination. Expert Rev Vaccines 2005;4(5):699–710.
[7] Tuyaerts S, Aerts JL, Corthals J, Neyns B, Heirman C, Breckpot K, et al. Current approaches in dendritic cell generation and future implications for cancer immunotherapy. Cancer Immunol Immunother 2007;56(10):1513–37.
[8] Lesterhuis WJ, Aarntzen EH, De Vries IJ, Schuurhuis DH, Figdor CG, Adema GJ, et al. Dendritic cell vaccines in melanoma: from promise to proof? Crit Rev Oncol Hematol 2008;66(2):118–34.
[9] Proudfoot O, Apostolopoulos V, Pietersz GA. Receptor-mediated delivery of antigens to dendritic cells: anticancer applications. Mol Pharm 2007;4(1):58–72.
[10] Arthur JF, Butterfield LH, Roth MD, Bui LA, Kiertscher SM, Lau R, et al. A comparison of gene transfer methods in human dendritic cells. Cancer Gene Ther 1997;4(1):17–25.
[11] Lotem M, Zhao Y, Riley J, Hwu P, Morgan RA, Rosenberg SA, et al. Presentation of tumor antigens by dendritic cells genetically modified with viral and nonviral vectors. J Immunother 2006;29(6):616–27.
[12] van Leeuwen EB, Cloosen S, Senden-Gijsbers BL, Germeraad WT, Bos GM. Transduction with a fiber-modified adenoviral vector is superior to non-viral nucleofection for expressing tumor-associated Ag mucin-1 in human DC. Cytotherapy 2006;8(1):36–46.
[13] Zhong L, Granelli-Piperno A, Choi Y, Steinman RM. Recombinant adenovirus is an efficient and non-perturbing genetic vector for human dendritic cells. Eur J Immunol 1999;29(3):964–72.
[14] Zhang L, Tang Y, Akbulut H, Zelterman D, Linton PJ, Deisseroth AB. An adenoviral vector cancer vaccine that delivers a tumor-associated antigen/CD40-ligand fusion protein to dendritic cells. Proc Natl Acad Sci USA 2003;100(25):15101–6.
[15] Cho HI, Kim HJ, Oh ST, Kim TG. In vitro induction of carcinoembryonic antigen (CEA)-specific cytotoxic T lymphocytes by dendritic cells transduced with recombinant adenoviruses. Vaccine 2003;22(2):224–36.
[16] Noureddini SC, Curiel DT. Genetic targeting strategies for adenovirus. Mol Pharm 2005;2(5):341–7.
[17] Tillman BW, de Gruijl TD, Luykx-de Bakker SA, Scheper RJ, Pinedo HM, Curiel TJ, et al. Maturation of dendritic cells accompanies high-efficiency gene transfer by a CD40-targeted adenoviral vector. J Immunol 1999;162(11):6378–83.
[18] Pereboev AV, Nagle JM, Shakhmatov MA, Triozzi PL, Matthews QL, Kawakami Y, et al. Enhanced gene transfer to mouse dendritic cells using adenoviral vectors coated with a novel adapter molecule. Mol Ther 2004;9(5):712–20.
[19] Izumi M, Kawakami Y, Glasgow JN, Belousova N, Everts M, Kim-Park S, et al. In vivo analysis of a genetically modified adenoviral vector targeted to human CD40 using a novel transient transgenic model. J Gene Med 2005;7(12):1517–25.
[20] Korokhov N, Noureddini SC, Curiel DT, Santegoets SJ, Scheper RJ, de Gruijl TD. A single-component CD40-targeted adenovirus vector displays highly efficient transduction and activation of dendritic cells in a human skin substrate system. Mol Pharm 2005;2(3):218–23.
[21] Belousova N, Korokhov N, Krendelshchikova V, Simonenko V, Mikheeva G, Triozzi PL, et al. Genetically targeted adenovirus vector directed to CD40-expressing cells. J Virol 2003;77(21):11367–77.
[22] Clement A, Pereboev A, Curiel DT, Dong SS, Hutchings A, Thomas JM. Converting nonhuman primate dendritic cells into potent antigen-specific cellular immunosuppressants by genetic modification. Immunol Res 2002;26(1–3):297–302.
[23] de Gruijl TD, Luykx-de Bakker SA, Tillman BW, van den Eertwegh AJ, Buter J, Lougheed SM, et al. Prolonged maturation and enhanced transduction of dendritic cells migrated from human skin explants after in situ delivery of CD40-targeted adenoviral vectors. J Immunol 2002;169(9):5322–31.
[24] Pereboev AV, Asiedu CK, Kawakami Y, Dong SS, Blackwell JL, Kashentseva EA, et al. Coxsackievirus-adenovirus receptor genetically fused to anti-human CD40 scFv enhances adenoviral transduction of dendritic cells. Gene Ther 2002;9(17):1189–93.
[25] Huang D, Pereboev AV, Korokhov N, He R, Larocque L, Gravel C, et al. Significant alterations of biodistribution and immune responses in Balb/c mice administered with adenovirus targeted to CD40(+) cells. Gene Ther 2008;15(4):298–308.
[26] Paoloni M, Khanna C. Translation of new cancer treatments from pet dogs to humans. Nat Rev Cancer 2008;8(2):147–56.
[27] Khanna C, Lindblad-Toh K, Vail D, London C, Bergman P, Barber L, et al. The dog as a cancer model. Nat Biotechnol 2006;24(9):1065–6.
[28] Porrello A, Cardelli P, Spugnini EP. Oncology of companion animals as a model for humans. An overview of tumor histotypes. J Exp Clin Cancer Res 2006;25(1):97–105.
[29] Waters DJ, Wildasin K. Cancer clues from pet dogs. Sci Am 2006;295(6):94–101.
[30] Smith BF, Baker HJ, Curiel DT, Jiang W, Conry RM. Humoral and cellular immune responses of dogs immunized with a nucleic acid vaccine encoding human carcinoembryonic antigen. Gene Ther 1998;5(7):865–8.
[31] Casal M, Haskins M. Large animal models and gene therapy. Eur J Hum Genet 2006;14(3):266–72.
[32] Seki T, Dmitriev I, Kashentseva E, Takayama K, Rots M, Suzuki K, et al. Artificial extension of the adenovirus fiber shaft inhibits infectivity in coxsackievirus and adenovirus receptor-positive cell lines. J Virol 2002;76(3):1100–8.
[33] Krasnykh V, Belousova N, Korokhov N, Mikheeva G, Curiel DT. Genetic targeting of an adenovirus vector via replacement of the fiber protein with the phage T4 fibritin. J Virol 2001;75(9):4176–83.
[34] Graham FL, Prevec L. Methods for construction of adenovirus vectors. Mol Biotechnol 1995;3(3):207–20.
[35] Oster W, Lindemann A, Mertelsmann R, Herrmann F. Regulation of gene expression of M-, G-, GM-, and multi-CSF in normal and malignant hematopoietic cells. Blood Cells 1988;14(2–3):443–62.
[36] Lu L, Srour EF, Warren DJ, Walker D, Graham CD, Walker EB, et al. Enhancement of release of granulocyte- and granulocyte-macrophage colony-stimulating factors from phytohemagglutinin-stimulated sorted subsets of human T lymphocytes by recombinant human tumor necrosis factor-alpha. Synergism with recombinant human IFN-gamma. J Immunol 1988;141(1):201–7.

[37] Krasnykh VN, Mikheeva GV, Douglas JT, Curiel DT. Generation of recombinant adenovirus vectors with modified fibers for altering viral tropism. J Virol 1996;70(10):6839–46.
[38] Perreau M, Mennechet F, Serratrice N, Glasgow JN, Curiel DT, Wodrich H, et al. Contrasting effects of human, canine, and hybrid adenovirus vectors on the phenotypical and functional maturation of human dendritic cells: implications for clinical efficacy. J Virol 2007;81(7):3272–84.
[39] Korokhov N, Mikheeva G, Krendelshchikov A, Belousova N, Simonenko V, Krendelshchikova V, et al. Targeting of adenovirus via genetic modification of the viral capsid combined with a protein bridge. J Virol 2003;77(24):12931–40.
[40] Bajorath J, Chalupny NJ, Marken JS, Siadak AW, Skonier J, Gordon M, et al. Identification of residues on CD40 and its ligand which are critical for the receptor-ligand interaction. Biochemistry 1995;34(6):1833–44.
[41] Bajorath J. Detailed comparison of two molecular models of the human CD40 ligand with an X-ray structure and critical assessment of model-based mutagenesis and residue mapping studies. J Biol Chem 1998;273(38):24603–9.
[42] Weber LW, Bowne WB, Wolchok JD, Srinivasan R, Qin J, Moroi Y, et al. Tumor immunity and autoimmunity induced by immunization with homologous DNA. J Clin Invest 1998;102(6):1258–64.
[43] Gold JS, Ferrone CR, Guevara-Patino JA, Hawkins WG, Dyall R, Engelhorn ME, et al. A single heteroclitic epitope determines cancer immunity after xenogeneic DNA immunization against a tumor differentiation antigen. J Immunol 2003;170(10):5188–94.
[44] Naftzger C, Takechi Y, Kohda H, Hara I, Vijayasaradhi S, Houghton AN. Immune response to a differentiation antigen induced by altered antigen: a study of tumor rejection and autoimmunity. Proc Natl Acad Sci USA 1996;93(25):14809–14.
[45] Hawkins WG, Gold JS, Dyall R, Wolchok JD, Hoos A, Bowne WB, et al. Immunization with DNA coding for gp100 results in CD4 T-cell independent antitumor immunity. Surgery 2000;128(2):273–80.
[46] Mahnke K, Qian Y, Fondel S, Brueck J, Becker C, Enk AH. Targeting of antigens to activated dendritic cells in vivo cures metastatic melanoma in mice. Cancer Res 2005;65(15):7007–12.
[47] Hauser H, Shen L, Gu QL, Krueger S, Chen SY. Secretory heat-shock protein as a dendritic cell-targeting molecule: a new strategy to enhance the potency of genetic vaccines. Gene Ther 2004;11(11):924–32.
[48] Bonifaz LC, Bonnyay DP, Charalambous A, Darguste DI, Fujii S, Soares H, et al. In vivo targeting of antigens to maturing dendritic cells via the DEC-205 receptor improves T cell vaccination. J Exp Med 2004;199(6):815–24.
[49] Yang L, Yang H, Rideout K, Cho T, Joo KI, Ziegler L, et al. Engineered lentivector targeting of dendritic cells for in vivo immunization. Nat Biotechnol 2008;26(3):326–34.
[50] Kretz-Rommel A, Qin F, Dakappagari N, Torensma R, Faas S, Wu D, et al. In vivo targeting of antigens to human dendritic cells through DC-SIGN elicits stimulatory immune responses and inhibits tumor growth in grafted mouse models. J Immunother 2007;30(7):715–26.
[51] Pereira CF, Torensma R, Hebeda K, Kretz-Rommel A, Faas SJ, Figdor CG, et al. In vivo targeting of DC-SIGN-positive antigen-presenting cells in a nonhuman primate model. J Immunother 2007;30(7):705–14.
[52] Mossoba ME, Medin JA. Cancer immunotherapy using virally transduced dendritic cells: animal studies and human clinical trials. Expert Rev Vaccines 2006;5(5):717–32.
[53] Basak SK, Kiertscher SM, Harui A, Roth MD. Modifying adenoviral vectors for use as gene-based cancer vaccines. Viral Immunol 2004;17(2):182–96.
[54] Molinier-Frenkel V, Lengagne R, Gaden F, Hong SS, Choppin J, Gahery-Segard H, et al. Adenovirus hexon protein is a potent adjuvant for activation of a cellular immune response. J Virol 2002;76(1):127–35.
[55] Banchereau J. The long arm of the immune system. Sci Am 2002;287(5):52–9.
[56] Finkelman FD, Lees A, Birnbaum R, Gause WC, Morris SC. Dendritic cells can present antigen in vivo in a tolerogenic or immunogenic fashion. J Immunol 1996;157(4):1406–14.
[57] Mackey MF, Gunn JR, Maliszewsky C, Kikutani H, Noelle RJ, Barth Jr RJ. Dendritic cells require maturation via CD40 to generate protective antitumor immunity. J Immunol 1998;161(5):2094–8.
[58] Day MJ, Immunoglobulin. G subclass distribution in canine leishmaniosis: a review and analysis of pitfalls in interpretation. Vet Parasitol 2007;147(1–2):2–8.
[59] Carvalho LH, Sano G, Hafalla JC, Morrot A, Curotto de Lafaille MA, Zavala F. IL-4-secreting CD4+ T cells are crucial to the development of CD8+ T-cell responses against malaria liver stages. Nat Med 2002;8(2):166–70.
[60] Boag PR, Parsons JC, Presidente PJ, Spithill TW, Sexton JL. Characterisation of humoral immune responses in dogs vaccinated with irradiated *Ancylostoma caninum*. Vet Immunol Immunopathol 2003;92(1–2):87–94.
[61] Fujiwara RT, Loukas A, Mendez S, Williamson AL, Bueno LL, Wang Y, et al. Vaccination with irradiated *Ancylostoma caninum* third stage larvae induces a Th2 protective response in dogs. Vaccine 2006;24(4):501–9.
[62] Breathnach RM, Fanning S, Mulcahy G, Bassett HF, Jones BR, Daly P. Evaluation of Th1-like, Th2-like and immunomodulatory cytokine mRNA expression in the skin of dogs with immunomodulatory-responsive lymphocytic–plasmacytic pododermatitis. Vet Dermatol 2006;17(5):313–21.
[63] Horiuchi Y, Hanazawa A, Nakajima Y, Nariai Y, Asanuma H, Kuwabara M, et al. T-helper (Th)1/Th2 imbalance in the peripheral blood of dogs with malignant tumor. Microbiol Immunol 2007;51(11):1135–8.

Enhanced Antitumor Effects of an Engineered Measles Virus Edmonston Strain Expressing the Wild-type *N*, *P*, *L* Genes on Human Renal Cell Carcinoma

Xin Meng[1,2], Takafumi Nakamura[3,4], Toshihiko Okazaki[1], Hiroyuki Inoue[1], Atsushi Takahashi[1], Shohei Miyamoto[1], Gaku Sakaguchi[5], Masatoshi Eto[5], Seiji Naito[5], Makoto Takeda[6], Yusuke Yanagi[6] and Kenzaburo Tani[1]

[1]Department of Molecular Genetics, Medical Institute of Bioregulation, Kyushu University, Fukuoka, Japan; [2]Department of Biochemistry and Molecular Biology, China Medical University, Shenyang, China; [3]Core Facility for Therapeutic Vectors, The Institute of Medical Science, The University of Tokyo, Tokyo, Japan; [4]RNA and Biofunctions, PRESTO, Japan Science and Technology Agency, Saitama, Japan; [5]Department of Urology, Graduate School of Medical Sciences, Kyushu University, Fukuoka, Japan; [6]Department of Virology, Faculty of Medicine, Kyushu University, Fukuoka, Japan

Measles virus Edmonston strain (MV-Edm) is thought to have remarkable oncolytic activity that selectively destroys human tumor cells. The P/V/C protein of wild-type MV was shown to resist the antiviral effects of interferon (IFN)-α. Here, we engineered new MVs by arming MV-Edm tag strain (a V-defective vaccine-lineage strain, MV-Etag) with the *P* or *N*, *P*, and *L* genes of wild-type MV (MV-P and MV-NPL, respectively). The oncolytic activities of the MVs were determined in human renal cell carcinoma (RCC) cell lines and primary human RCC cells by the MTT assay. The antitumor efficacy of the MVs was evaluated in A-498 xenografts in nude mice. IFN-α effectively inhibited the replication of MV-Etag and MV-P, but not MV-NPL. MV-NPL more efficiently induced cytopathic effects (CPEs) in OS-RC-2 cells, even in the presence of human IFN-α. MV-NPL replicated more rapidly than MV-P and MV-Etag in A-498 cells. Apoptosis was induced earlier in A-498 cells by MV-NPL than MV-Etag and MV-P. MV-NPL showed more significant antitumoral effects and had prolonged replication compared to MV-Etag and MV-P. In this study, we demonstrated that the newly engineered MV-NPL has more effective oncolytic activity and may help establish an innovative cancer therapy.

Received 31 August 2009; accepted 2 December 2009; advance online publication 5 January 2010. doi:10.1038/mt.2009.296

INTRODUCTION

Oncovirotherapy, which uses replication-competent viruses as a cancer therapy, is attracting much interest.[1–4] Recently, several reports confirmed that these live-attenuated viruses can induce rapid and lytic infections in tumor cells.[5–10] Furthermore, some viruses are being used as cancer therapies in current clinical trials.[4,11,12] Measles virus Edmonston strain (MV-Edm) has potent antineoplastic activity against various human cancers, including lymphoma, ovarian cancer, mesothelioma, breast cancer, and hepatocellular carcinoma.[11,13–16] It selectively induces potent cytopathic effects (CPEs), notably intercellular fusion in cancer cells, but causes minimal damage in normal cells.[9,17] In addition, the MV genome is very stable and the vaccine strains have never reverted to pathogenic forms, making MV highly suitable for further development as an oncolytic agent.

Measles virus is a negative-strand RNA virus of the Morbillivirus genus in the *Paramyxoviridae* family. A polymerase (L) and its cofactor (P) associate with the viral RNA and N protein to form a ribonucleoprotein. This complex is surrounded by the M protein. The *P* gene encodes the P protein and two nonstructural accessory proteins, C and V.[18] The two MV envelope glycoproteins H and F work in concert to induce virus–cell membrane fusion. CD46 and CD150 were identified as two MV receptors. CD150 expression is confined to immune cells, whereas CD46 is expressed ubiquitously in nucleated cells.[19–21] CD46 is abundantly expressed in cancer cells,[22,23] but minimally expressed in normal cells such as fibroblasts and peripheral blood lymphocytes,[9,17] making cancer cells a suitable target for MV oncolytic therapy.

Type I interferon (IFN-α/β) is a powerful innate antiviral defense. MV vaccine strains can induce significantly higher levels of type I IFN than wild-type MV.[24] To combat the cellular innate immune response, many viruses encode antagonistic molecules that block some steps of the type I IFN antiviral response.[25] The P proteins of wild-type MV have been shown to resist type I IFN. Furthermore, an engineered MV-Edm tag strain (MV-P), whose *P* gene was replaced with the comparable wild-type gene, induces significantly less IFN-α in tumor cells and has enhanced oncolytic potency against human multiple myeloma compared to the parental virus.[13] The major function of the N protein is to surround the genomic RNA, encapsidate the viral genome, and support

Correspondence: Kenzaburo Tani, Department of Molecular Genetics Medical Institute of Bioregulation, Kyushu University, Fukuoka 812-8582, Japan. E-mail: taniken@bioreg.kyushu-u.ac.jp

its replication and transcription.[26,27] The N, P, and L proteins are assembled into the ribonucleoprotein, which is the viral replication unit. Therefore, we reasoned that combining a safe targeted therapy mechanism that destroys the host antiviral genetic program and enhances viral genome replication in cancer cells would generate a novel and innovative cancer gene therapy.

In this study, we generated a newly engineered MV, MV-NPL, which is based on the Edm tag strain but is armed with the *N*, *P*, and *L* genes of the wild-type strain. We demonstrated that MV-NPL has enhanced oncolytic activity against human renal cell carcinoma (RCC) cell lines *in vitro* and *in vivo* compared to MV-Edm tag and MV-P. We found that MV-NPL had faster replication and transcription than MV-Edm tag and MV-P in RCC cell lines *in vitro* and RCC cell line xenografts *in vivo*. In addition, MV-NPL efficiently proliferated and killed RCC cell line even in the presence of IFN-α. Furthermore, this oncolytic activity was specific as MV-NPL caused minimal cytopathic effects in normal human cell line.

RESULTS

CD46 is overexpressed in human RCC cell lines

CD46 expression in the human RCC cell lines A-498 and OS-RC-2, primary human RCC cells of T5, normal human skin fibroblast cell line BJ-1 was analyzed by flow cytometry. CD46 was expressed on the surface of most human RCC cell lines and primary human RCC cells: 93.8% in A-498, 93.7% in OS-RC-2, and 92–95% in primary human RCC cells (n = 3). However, only 8.7% in BJ-1 demonstrated positive expression of CD46 (**Figure 1**). These results demonstrated that human RCC cell lines and primary RCC cells expressed higher levels of CD46 than normal cells.

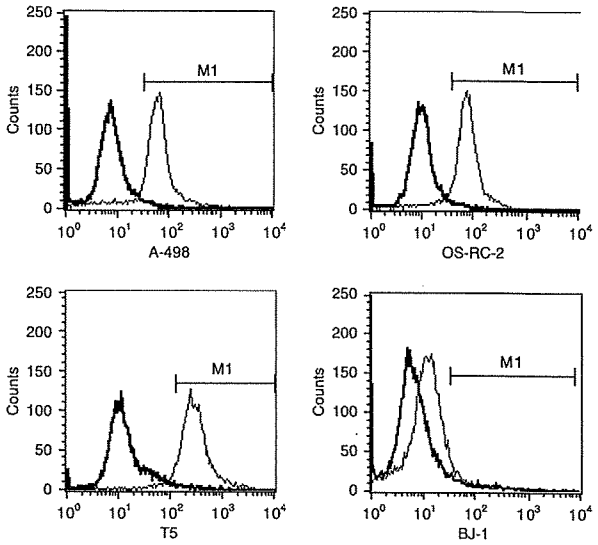

Figure 1 CD46 receptor expression on the human renal cell carcinoma (RCC) cell lines A-498 and OS-RC-2, primary human RCC cells of T5, and normal human cell line BJ-1. CD46 receptor was highly expressed on the human RCC cell lines A-498 and OS-RC-2 as well as primary human RCC cells of T5, but was minimally expressed on the normal human cell line BJ-1. The analysis was performed by flow cytometry. CD46 expression in isotype control is 1%. The thick histograms show the measured fluorescence of cells incubated with an isotype control (detailed) and the thin histograms represent cells labeled with an anti-CD46 fluorescein isothiocyanate antibody.

MV-NPL induces stronger CPEs than MV-P and MV-Etag in human RCC cell lines and primary human RCC cells

Schematic representation of the genome of MV-Etag (a V-defective vaccine-lineage strain) strain, engineered MV-Etag strain that expresses the wild-type *P* gene (MV-P) and the engineered MV-Etag strain that expresses the wild-type *N*, *P*, and *L* genes (MV-NPL) is shown in **Figure 2a**. They were rescued and efficiently propagated in Vero cells and used for the following experiments. We studied the CPEs associated with each MV in the human RCC cell lines A-498 and OS-RC-2, primary RCC cells (n = 3), the normal human skin fibroblast cell line BJ-1. Cells were infected with the various viruses at multiplicities of infection (MOIs) of 1 and 0.1 for 120 hours and the stained with crystal violet. Compared to MV-P and MV-Etag, MV-NPL demonstrated more dramatic CPEs in an MOI-dependent manner (n = 3; **Figure 2b**). The CPEs appeared at 72 hours postinfection with each MV at an MOI of 0.1 in both A-498 and OS-RC-2 cells and primary RCC cells (data not shown). However, normal human cell line BJ-1 showed minimal CPEs after each MV infection (**Figure 2b**). We further determined the cell viability after infection with the various viruses using the Cell-Titer 96 Aqueous Non-Radioactive Cell Proliferation Assay. Analyses were performed every 24 hour for 120 hours. Compared with MV-P and MV-Etag, MV-NPL demonstrated a greater reduction of proliferation in A-498, OS-RC-2, and primary RCC cells from 72 or 96 hours to 120 hours at an MOI of 0.1 (n = 3; **Figure 2c**).

MV-NPL induces faster cell lysis in A-498 cells than MV-P and MV-Etag

A-498 cells were plated in 6-well plates at a density of 2×10^5 cells/well. The cells were infected with various viruses at an MOI of 0.1 and the supernatants and cells were collected from 12 to 120 hours. The intracellular viruses were released by two cycles of freezing/thawing. The viral titers were determined as the TCID50 (50% tissue culture infective dose) in Vero cells in a 96-well plate. The intracellular MV-NPL viral titer of A-498 cells peaked at 60 hours postinfection (**Figure 3a**). Compared with MV-NPL, intracellular MV-P virus demonstrated slower replication and the viral titer peaked at 84 hours (**Figure 3a**). In the culture supernatant, the MV-NPL viral titer peaked at 72 hours (**Figure 3b**). Similar to the intracellular viral titer, the extracellular MV-P titer peaked with delayed kinetics at 84–96 hours compared to MV-NPL. We also found that after the intracellular viral titer peaked, the viral titer in the culture supernatant peaked in A-498 cells infected with MV-NPL. Real-time RT-PCR analyses revealed a time-dependent increase in measles viral mRNA in A-498 cells, and compared with other viruses, cells infected with MV-NPL demonstrated higher viral mRNA levels (**Figure 3c**).

MVs induced human IFN-α production from human normal skin fibroblast cells of BJ-1, and human RCC cells of A-498 and OS-RC-2. MV-NPL more effectively evaded to the antiviral defense of IFN-α in Vero cells than MV-P and MV-Etag.

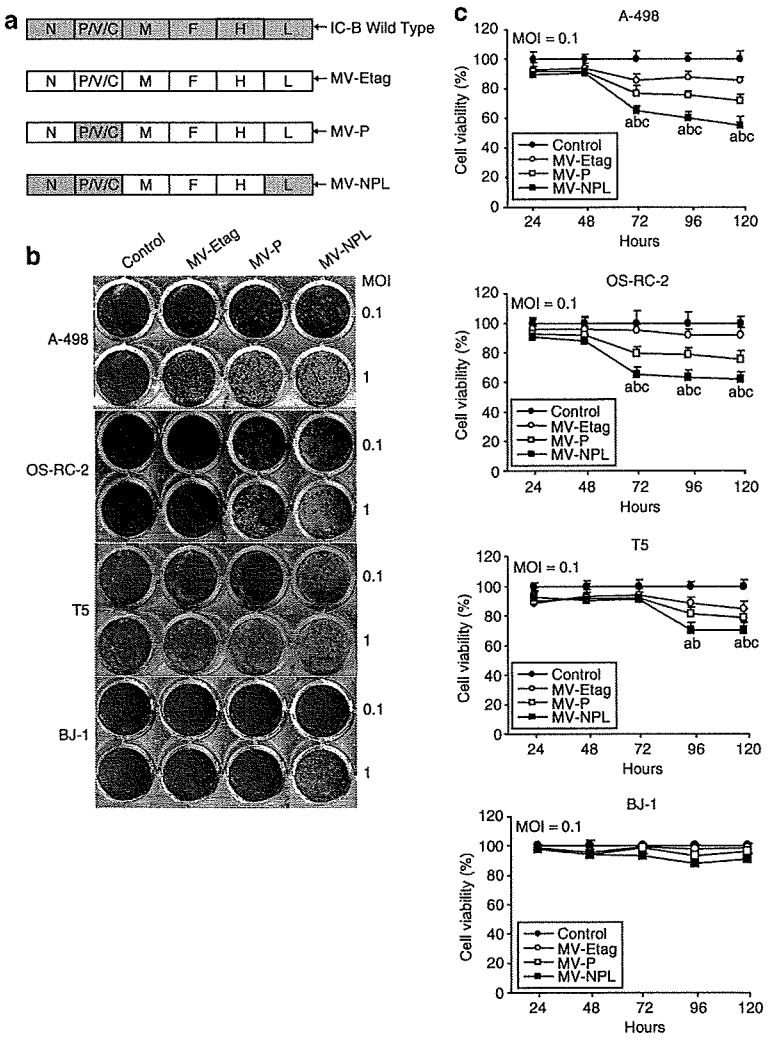

Figure 2 Induction of cytopathic effects (CPEs) and cell death in human renal cell carcinoma (RCC) cell lines A-498, OS-RC-2, primary RCC cells T5, and normal human cell line BJ-1 by MV-Etag, MV-P, and MV-NPL. (**a**) At 120 hours after infection with each MV at multiplicities of infection (MOIs) of 1 and 0.1, the cells were stained with crystal violet. (**b**) Cells were infected with each MV at an MOI of 0.1 and cell viability was analyzed using the MTT assay. Each value is normalized to the control (untreated cells), which was set at 100%, and represents the mean ± SD (**a**, $P < 0.01$, MV-NPL versus control group; **b**, $P < 0.01$, MV-NPL versus MV-Etag group; **c**, $P < 0.01$, MV-NPL versus MV-P group).

The IFN family, particularly type I IFN (IFN-α/β), induces a powerful innate antiviral response. IFN-α production induced by human normal and tumor cells after infection by MVs was quantified using IFN-specific enzyme-linked immunosorbent assay (ELISA) kits (**Figure 4a**). We examined the sensitivity of the MV viruses to human IFN-α. Vero cells were infected with different MVs at an MOI of 0.001, and then treated with human IFN-α (1,000 IU/ml) 2 hours after infection. The viral titers were determined at 48 hours postinfection. Human IFN-α effectively inhibited MV-Etag proliferation (**Figure 4b**). To some extent, IFN-α also suppressed MV-P proliferation, whereas it had no apparent effect on MV-NPL proliferation (**Figure 4b**). To investigate whether IFN-α can prevent the CPEs of MV, OS-RC-2 cells were infected with each MV at an MOI of 0.1. Different concentrations of human IFN-α (250–2,000 IU/ml) were added to the infected cells and crystal violet staining was performed at 120 hours after infection. Compared to MV-P and MV-Etag, MV-NPL more effectively induced CPE even in the presence of IFN-α. However, there were no obvious CPEs in BJ-1 cells (**Figure 4c**).

MV-NPL induces more apoptosis in human RCC cells than MV-P and MV-Etag

A-498 cells were infected with each MV at an MOI of 0.1, and apoptotic cells were analyzed by propidium iodide staining and subsequent flow cytometry. Upon infection with the MVs, the number of cells in sub-G1 increased in a time-dependent manner (**Figure 5a**). MV-NPL induced apoptosis in ~20 and 40% of cells at 48 and 72 hours at an MOI of 0.1, respectively (**Figure 5a**). However, at the same time points, MV-P and MV-Etag only induced apoptosis in ~10 and 15% of cells (**Figure 5a**). We further examined poly(ADP-ribose) polymerase expression and found that the 85-kd cleaved poly(ADP-ribose) polymerase fragment

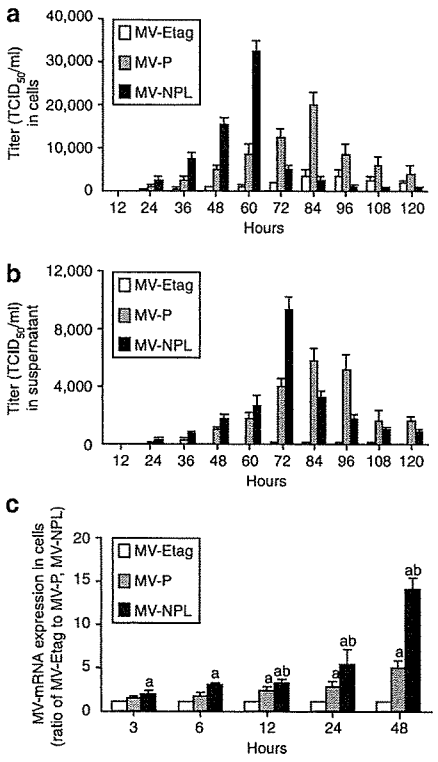

Figure 3 Production of MV-Etag, MV-P, or MV-NPL in the human renal cell carcinoma (RCC) cell line A-498. Cells were infected with each MV at an multiplicity of infection (MOI) of 0.1. (**a**) Cells and (**b**) supernatants were harvested at the indicated times. The viral titers were determined on Vero cells and expressed as $TCID_{50}$/ml. (**c**) Total RNA from A-498 cells was isolated at the indicated times. The viral mRNA levels were measured using real-time PCR. Each value is normalized to that in MV-Etag, which was set a ratio = 1, and represents the mean ± SD (**a**, $P < 0.05$, MV-NPL and MV-P versus MV-Etag; **b**, $P < 0.05$, MV-NPL versus MV-P). $TCID_{50}$, 50% tissue culture infective dose.

(85 kd) was more rapidly expressed in A-498 cells infected with MV-NPL than those infected with MV-P or MV-Etag (**Figure 5b**).

Intratumoral administration of MV-NPL induces regression of A-498 xenografts

Each MV was given intratumorally to nude mice bearing established (0.5–0.6 cm in diameter) subcutaneous human A-498 tumor xenografts. Intratumoral administration of MV-Etag or MV-P (10 doses of 1.0×10^5 $TCID_{50}$/dose) effectively suppressed the growth of A-498 xenografts. Compared with MV-Etag or MV-P, intratumoral injection of MV-NPL caused even more regression of the A-498 xenografts (**Figure 6a**). At 80 days after injection, the survival rate was significantly improved in the MV-NPL-injected group (55%), compared to the control group (0%), MV-Etag-injected group (0%), and MV-P-injected group (11%) (**Figure 6b**). A-498 xenografts infected with MV-NPL had the highest mRNA expression of the *M* gene of MV, indicating that MV-NPL was more effectively replicated in the xenografts than MV-P at 19 days after the injection when the former significantly suppressed the tumor growth than the latter ($P < 0.05$) (**Figure 6c**).

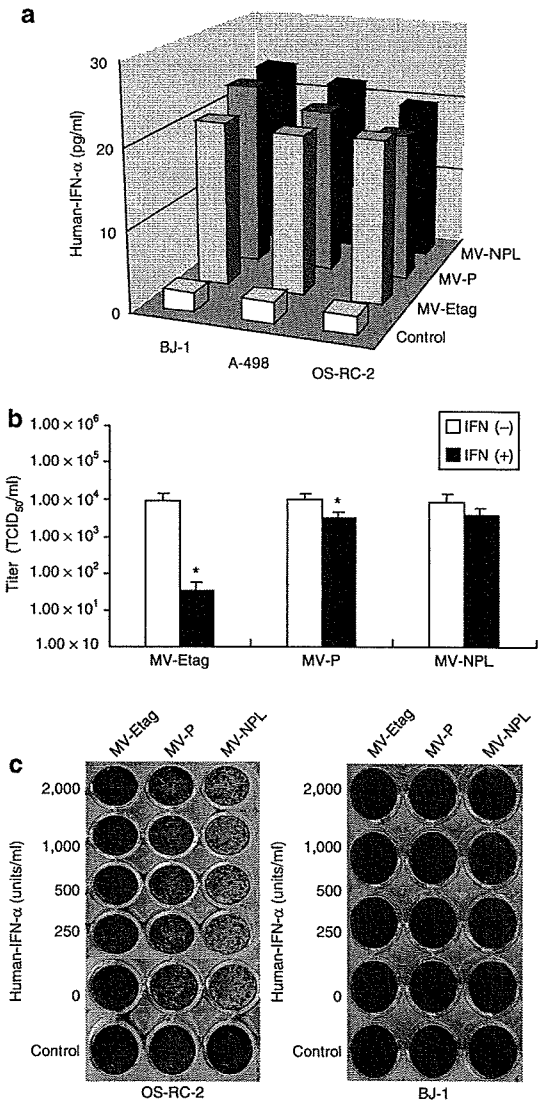

Figure 4 Different sensitivities of MV-Etag, MV-P, and MV-NPL to human INF-α. (**a**) BJ-1, A-498 and OS-CR-2 cells were infected with MV-Etag, MV-P, or MV-NPL at an multiplicity of infection (MOI) of 0.1. After 48-hour infection, the production of IFN-α was determined using human IFN-α enzyme-linked immunosorbent assay kit. (**b**) Vero cells were infected with each MV at an MOI of 0.001 and cultured in the presence or absence of 1,000 IU/ml recombinant IFN-α. Viral titers at 48 hours were determined by titrating the TCID50 on Vero cells, $*P < 0.05$ versus IFN(+). (**c**) OS-RC-2 cells and BJ-1 cells in 24-well plates were infected with each MV at an MOI of 0.1. Two hours after infection, human IFN-α was added to the cells at the indicated concentrations. At 120 hours after infection, the cells were stained with crystal violet. IFN, interferon; $TCID_{50}$, 50% tissue culture infective dose.

DISCUSSION

Oncovirotherapy using replication-competent viruses for cancer treatment has recently attracted considerable attention. Engineering replication-competent viruses for cancer therapy is a novel and promising strategy. Live-attenuated MV has a potent and tumor-specific oncolytic activity against a variety of human tumors.[9,13,28,29] In clinical trials, the MV vaccine strain has been shown to mediate regression of T-cell lymphomas when administered intratumorally.[11]

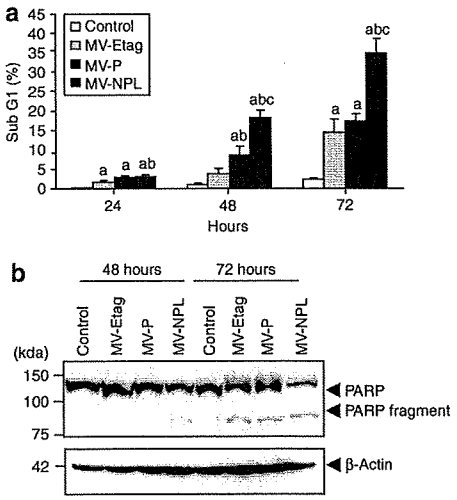

Figure 5 Apoptosis induced by MV-Etag, MV-P or MV-NPL in the human renal cell carcinoma (RCC) cell line A-498. Cells were infected with each MV at an multiplicity of infection (MOI) of 0.1. (**a**) Adherent and detached cells were harvested at 24, 48, and 72 hours postinfection. The percentage of sub-G1 cells was measured by fluorescence-activated cell sorting (**a**, $P < 0.05$, MV-NPL, MV-P and MV-Etag versus control; **b**, $P < 0.05$, MV-NPL and MV-P versus MV-Etag; **c**, $P < 0.05$, MV-NPL versus MV-P). (**b**) Whole-cell lysates of A-498 cells that were infected with each MV were subjected to western blot analysis using anti-PARP and β-actin antibodies. PARP, poly(ADP-ribose) polymerase.

However, there is no report on the oncolytic effects of measles virus on human RCCs. In this study, we report for the first time that measles virus has potent antitumor activity against human RCC cells *in vitro* and in *vivo*.

Numerous factors in the tumor microenvironment, such as the stromal architecture and surrounding innate immune system, could potentially restrict viral replication and spread *in vivo*.[30] Human type I IFNs such as IFN-α/β have been shown to inhibit gene expression and the production of progeny virions of the measles virus vaccine strain, including Edmonston tag strain.[31–33] In order to more effectively control tumor growth and eventually eradicate tumors by direct viral spread and oncolysis, an attenuated replication-competent virus must be able to evade the host innate immune response.[13,34] The P/V/C protein of the MV wild-type strain encoded by the *P* gene was shown to block IFN-α induced-signaling, allowing the virus to evade the innate immune response.[13,18,31,35,36] The N, P and L proteins assemble into the ribonucleoprotein, which serves as the MV replication unit. In our study, we found that wild-type N protein provided virus with resistance to IFN similar to P (data no shown). Moreover, the L protein gene of wild type can more effectively induce viral RNA and protein synthesis than vaccine strain.[37] In this study, we engineered a novel MV-Edm by replacing the *N*, *P*, and *L* genes with those of the wild-type MV strain to create a virus that rapidly replicates on human renal cancer cells. Compared to MV-P and MV-Etag, MV-NPL exhibited more efficient replication and a potent killing effect in human renal cancer cells *in vitro* and *in vivo*. In our study, we demonstrated that human IFN-α effectively inhibited the replication of MV-Etag and MV-P, but not MV-NPL, at an MOI of 0.001 in Vero cells *in vitro*. Furthermore, MV-NPL exhibited more efficient cytopathic effects than MV-Etag and MV-P in OS-RC-2 cells even in the presence of IFN-α.

Several mechanisms could account for the enhanced antitumoral effects of the engineered virus *in vitro*, such as faster replication kinetics, enhanced cell killing, or evasion of host antiviral mechanisms.[13,34] In this study, we demonstrated that MV-NPL replicated faster than MV-P and MV-Etag. In addition, RCCs infected with MV-NPL produced more viruses than those infected with MV-P or MV-Etag. Measles M mRNA was detected earlier in A-498 cells infected with MV-NPL than with MV-P or MV-Etag, which resulted in more substantial upregulation of viral protein production compared to the other viruses in a time-dependent manner (**Figure 3**). Therefore, we considered that the rapid oncolysis of cancer cells induced by MV-NPL is due to rapid viral mRNA transcription followed by abundant intracellular viral protein production and accelerated cancer cells lysis, causing the cells to necrose after viral infection. To determine the mechanism of MV-induced cell death, we used sub-G1 staining. Our results demonstrated that MV-NPL induced apoptosis in infected tumor cells faster than MV-Etag and MV-P. Therefore, we concluded that not only necrosis but also apoptosis was an important mode in MV-induced cell death.

MV has been shown to use two receptors, SLAM (CD150) and CD46, for entry into cells. SLAM (CD150) is a signaling lymphocyte activation molecule and its expression profile is confined to immune cells. CD46 is ubiquitously expressed in nucleated cells. The MV-Edm strain can infect cells via CD46, which is expressed more frequently in human cancer cells than normal cells. The most important issue to consider when developing an effective oncovirotherapy is that the oncolytic virus needs to selectively infect tumor cells but not normal cells. Our data demonstrated that CD46 was overexpressed in human RCC cell lines as well as cultured primary human RCC cells with 11-fold higher expression than in the normal human BJ-1 cell line. Compared to cancer cells, MV induces minimal CPEs in normal human cell line. These results suggested that cancer cells are suitable targets for MV infection.

Compared with oncolytic DNA viruses, RNA viruses do not require host nuclear transcription factors, and must rely on an alternative mechanism to preferentially replicate in tumor cells.[30] Furthermore, the MV genome is very stable, and the vaccine strains have never reverted to pathogenic forms. The Edmonston strain has been successfully used as a vaccine with an excellent safety profile. These data suggest that the MV vaccine strain has high tumor selectivity and safety, even though additional safety studies should be performed before starting clinical trials. In this study, we demonstrated that even low intratumoral doses of the engineered MV *in vivo* are sufficient to induce tumor regression.

We also demonstrated that MV-NPL efficiently induced tumor regression and showed the highest viral mRNA expression in the mouse model compared to MV-Etag and MV-P. The oncolysis of cancer cells has been clearly shown *in vitro*, so we suspected that the same mechanism occurs in our *in vivo* model. In current oncolytic virus research, intratumoral, intravenous, or intraperitoneal injections have been used to treat immune-deficient mice bearing human tumor xenografts. Among these treatments, intratumorally injected virus can efficiently escape circulating

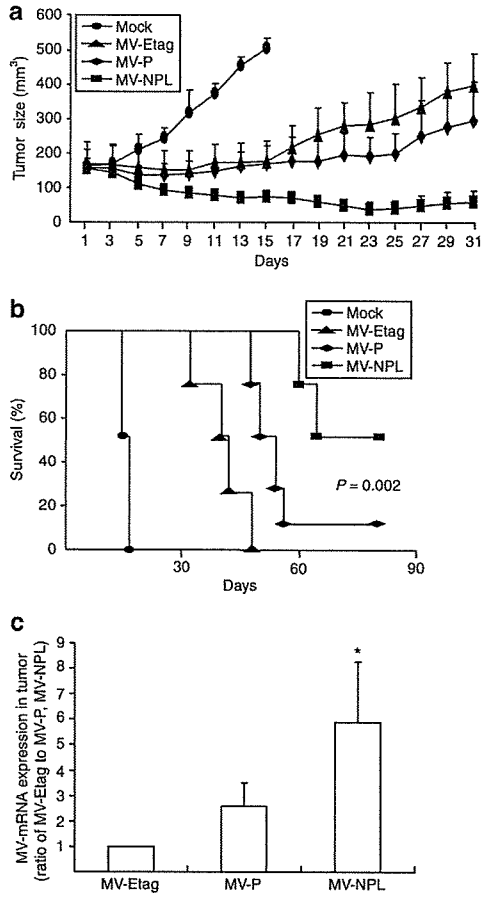

Figure 6 Therapeutic efficacy of MV-Etag, MV-P, or MV-NPL for renal cell carcinoma (RCC) xenografts *in vivo*. (**a**) A-498 cells (5×10^6 in 100 µl phosphate-buffered saline) were injected subcutaneously. When tumors reached a diameter of 0.5–0.6 cm, the virus was injected intratumorally every other day for a total of 10 doses (1.0×10^5 $TCID_{50}$/dose) over 19 days. The first day of injection represents day 1, and the tumor volumes were measured every other day ($n = 9$/group). (**b**) Kaplan–Meier survival analysis are shown for treated mice and mock-treated mice ($P = 0.002$, MV-NPL versus MV-P). (**c**) Intratumoral administration of each MV was initiated with a 1.0×10^5 $TCID_{50}$ injection. Nineteen days after injection, the tumors were harvested and the *M* gene viral mRNA levels were determined by real-time PCR, $^*P < 0.05$ versus MV-P. $TCID_{50}$, 50% tissue culture infective dose.

MV–neutralizing antibodies; therefore, this method is considered to be more desirable.

Currently, some additional immune mechanisms have been implicated in oncovirotherapy-mediated therapeutic effects. Several studies have shown that CD8 T cells are related to the efficiency of herpes simplex virus–induced,[38] vesicular stomatitis virus–induced,[39] and MV-induced[14,40] virotherapies. However, adult patients infected with measles virus have significantly higher levels of regulatory T cells, IFN-γ, and interleukin-10 (ref. 41). Furthermore, the phagocytosis of apoptotic MV-infected mesothelioma cells induced spontaneous DC maturation and activation and significant CD8 T-cell amplification. Collectively, oncovirotherapy may exhibit multiple clinical effects, including tumor lysis followed by the appearance and persistence of antitumor immunity.

In summary, our current results demonstrated that newly engineered MV-NPL has more effective oncolytic activity than the parental virus or MV-P as a systemic therapy for human RCC. The engineered virus caused CPEs in human RCCs, but had no toxic effects on normal human cells. Furthermore, MV-NPL replicated faster and more effectively resisted IFN-α than MV-Etag and MV-P, allowing the virus to escape the innate immune response. Although additional safety issues should be investigated, these properties of MV-NPL may help establish an innovative cancer therapy in the future.

MATERIALS AND METHODS

Construction of engineered viruses. The plasmids p(+)MV323 (ref. 42) and p(+)MV2A (ref. 43), which encode the full-length antigenomic complementary DNA of the IC-B wild-type strain and the Edmonston tag strain, respectively, were used in this study. We inserted restriction enzyme sites (*Sna*BI-N-*Spl*I-P-*Eco*47III-M-*Nru*I-F-*Pac*I-H-*Spe*I-L-*Pme*I) into the noncoding region of the p(+)MV323 genome using PCR with specific primers. Using the appropriate restriction enzymes, a series of genomic regions of p(+)MV2A were replaced with identical regions in p(+)MV323, which generated plasmids carrying the full-length genomes of recombinant engineered viruses (**Figure 3a**). Engineered MVs were rescued from cloned viral genome complementary DNA with a highly efficiently reverse genetics system as described previously.[44] The engineered MVs were propagated in Vero cells, an African green monkey kidney epithelial cell line, and passage three viral stocks were used in this study.

Cell line culture. The human RCC cell lines A-498 and OS-RC-2, the normal human skin fibroblast cell line BJ-1 were maintained in Dulbecco's modified Eagle's medium supplemented with 10% heat-inactivated fetal bovine serum (Japan Bioserum; Sigma, Steinheim, Germany). Vero cells were used to produce measles virus and maintained in Dulbecco's modified Eagle's medium supplemented with 5% heat-inactivated fetal bovine serum (Japan Bioserum). All media used in this study contained 100 U/ml of penicillin–streptomycin. All cell lines used in this study were cultured in a humidified atmosphere with 5% CO_2 at 37 °C.

Primary cell culture. Primary human RCC tissues were established using surgical specimens immediately after resection from Kyushu University Hospital after institutional review board approval and informed patient consent. Tissues were sliced, minced, treated with collagenase (GIBCO, Invitrogen, Carlsbad, CA) at 37 °C for 2 hours on a shaker, and then filtered through a nylon mesh (100-µm diameter) to obtain single cell suspensions. Harvested cells were cultured in Minimum Essential Medium α medium (GIBCO, Invitrogen) supplemented with 10% heat-inactivated fetal bovine serum (Hyclone, Logan, UT) and 4 µg/ml of Gentamicin Reagent Solution (GIBCO, Invitrogen). All cells used in this study were cultured in a humidified atmosphere with 5% CO_2 at 37 °C.

Flow cytometry. CD46 expression and the subdiploid status of cells (sub-G1) were determined by flow cytometry. To measure CD46 expression, the cells were harvested with Cell Dissociation Buffer (GIBCO, Invitrogen), washed twice with phosphate-buffered saline (PBS), and incubated with a fluorescein isothiocyanate–labeled monoclonal mouse anti-human CD46 or control antibodies (BD Biosciences, Pharmingen) for 1 hour on ice. The cells were washed twice with PBS and then 10,000 cells per sample were analyzed using a FACScan (BD Biosciences, San Jose, CA). For sub-G1, A-498 cells were plated in 6-well plates, and then treated with each MV at an MOI of 0.1. Adherent and detached cells were harvested at 24, 48, and 72 hours after infection and fixed in ice-cold 70% ethanol for at least 1 hour. Cell pellets were washed twice with PBS and then incubated for 30 minutes at room temperature in 1 ml PBS containing 50 µg propidium iodide (Sigma-Aldrich, St Louis, MO), 0.1% Triton X-100, 1 mmol/l

EDTA, and 0.5 mg RNaseA. After staining, 10,000 events per sample were analyzed using a FACScan (BD Biosciences). Fragmented apoptotic nuclei were recognized by their sub-G1 DNA content. The percentage of sub-G1 cells was recorded for each sample. All flow cytometry data were analyzed using the Mod Fit LT software (Verity Software House, Topsham, MN).

***Evaluation of CPEs* in vitro.** A-498, OS-RC-2, T5 (cultured primary human RCC cells), and BJ-1 cells were cultured in 24-well plates at a density of 2×10^4 cells/well. The cells were infected with each MV at an MOI of 1 or 0.1 in 0.2 ml of Opti-MEM I (GIBCO, Invitrogen) for 2 hours. The virus suspension was removed, and 1 ml of fresh medium was added to each well with or without the noted concentrations of human IFN-α. At 120 hours after infection, the cells were gently washed twice with PBS, and the remaining cells were fixed with 0.5% glutaraldehyde in PBS for 15 minutes. Then, cells were washed with PBS and stained with 0.1% crystal violet solubilized in 2% ethanol–distilled water. The stained product was subsequently washed twice with distilled water, air-dried, and then photographed.

Western blot analysis and ELISA. Infected cells were harvested and solubilized in a Nonidet P-40-based lysis buffer [20 mmol/l Tris (pH 7.4), 250 mmol/l NaCl, 1% Nonidet P-40, 1 mmol/l EDTA, 50 mg/ml leupeptin, and 1 mmol/l phenylmethylsulfonyl fluoride). After incubating on ice for 5 minutes, the cell lysates were clarified by centrifugation at 13,000*g* for 30 minutes at 4 °C. The protein concentrations in the lysates were quantified using Multiskan spectrum. The samples were separated on precast 4–12% gradient MOPS polyacrylamide gels (NOVEX, San Diego, CA), and then transferred to nitrocellulose membranes (BIO-RAD, Hercules, CA). The membranes were pretreated with Tris-buffered saline containing 5% dry milk and 0.05% Triton X-100 (TBST) for 1 hour at room temperature and then incubated with monoclonal antiproteolytic cleavage of poly(ADP-ribose) polymerase (Biovision, Mountain View, CA) and a rabbit anti-β-actin (CHEMICON International, Temecula, CA) antibodies for 1 hour at room temperature. After several washes in TBST, the membranes were probed with rabbit or mouse peroxidase-conjugated secondary antibodies (Santa Cruz Biotechnology, Santa Cruz, CA) at room temperature for 1 hour. After a final wash with TBST, the immune-reactivity of the blots was detected using an enhanced chemiluminescence detection system (Amersham, Piscataway, NJ). ELISA specific for IFN-α was performed using a human IFN-α ELISA kit (PBL Biomedical Laboratories) as per manufacturer's instructions.

Cell proliferation assay. The Cell-Titer 96 Aqueous Non-Radioactive Cell Proliferation Assay (Promega, Madison, WI) was used in this study. A-498, OS-RC-2, T5, and BJ-1 cells were plated in 96-well plates at a density of 1×10^4 cells/well. Twelve hours after seeding, the cells were infected with each MV at an MOI of 0.1 for different time intervals and then incubated with 20 µl of MTS reagent for 2 hours at 37 °C. The absorbance at 490 nm was recorded using an ELISA plate reader.

Assessment of MV replication in a human RCC cell line. The human RCC cell line A-498 was seeded in 6-well plates at a density of 2.0×10^4 cells/well. Twelve hours after plating, the cells were infected with each MV at an MOI of 0.1 in Opti-MEM I. The cells and supernatants were collected at different time intervals. The viruses were released by two cycles of freezing and thawing. The viral titers in the cells and supernatants were determined by titrating the TCID50 on Vero cells.

Human IFN-α sensitivity of MVs. Vero cells were infected with each MV at an MOI of 0.001. Two hours after infection, human IFN-α A/D (Sigma, St Louis, MO) was added to the cells at a concentration of 1,000 IU/ml. At 48 hours postinfection, the cells were harvested together with the culture media. The viral titers in both the intracellular samples and the culture supernatants were determined by titrating the TCID50 on Vero cells.

In vivo *xenograft experiments.* A-498 cells (5×10^6 in 100 µl PBS) were injected subcutaneously into the right flanks of 4-week-old female BALB/c nude mice using a 27-gauge needle. The length and width of the tumors in each mouse were measured daily with calipers. Mice were randomly divided into four groups: MV-Etag, MV-P, MV-NPL, or control (n = 9/group). Intratumoral administration of each MV was initiated when the tumors reached a diameter of 0.5–0.6 cm. The mice were injected with each MV (1×10^5 TCID50 in 50 µl Opti-MEM I), and each mouse received 10 MV doses on days 1, 3, 5, 7, 9, 11, 13, 15, 17, and 19. Control mice (mock therapy group) were injected with equal volumes of Opti-MEM I containing no virus. The tumor volume was calculated as length × width × width/2. Mice were killed if they lost >20% of their body weight or the tumor diameter exceeded 1.0 cm. All mouse experiments were approved by the Committee of the Ethics on Animal Experiments in the Faculty of Medicine, Kyushu University and carried out following the Guidelines for Animal Experiments in the Faculty of Medicine, Kyushu University, Fukuoka, Japan and The Law and Notification of the Government.

Statistical analysis. Each experiment was repeated three different times, and data are presented as means ± SD. Where indicated, the data were analyzed by a one-way analysis of variance with Bonferroni's *post hoc* test using SPSS 15.0 software (SPSS, Chicago, IL). P values <0.05 were considered statistically significant.

ACKNOWLEDGMENTS

This work was supported by a grant from the Ministry of Education, Culture, Sports, Science and Technology.

REFERENCES

1. Cattaneo, R, Miest, T, Shashkova, EV and Barry, MA (2008). Reprogrammed viruses as cancer therapeutics: targeted, armed and shielded. *Nat Rev Microbiol* **6**: 529–540.
2. Kirn, DH and Thorne, SH (2009). Targeted and armed oncolytic poxviruses: a novel multi-mechanistic therapeutic class for cancer. *Nat Rev Cancer* **9**: 64–71.
3. Liu, TC and Kirn, D (2008). Gene therapy progress and prospects cancer: oncolytic viruses. *Gene Ther* **15**: 877–884.
4. Aghi, M and Martuza, RL (2005). Oncolytic viral therapies—the clinical experience. *Oncogene* **24**: 7802–7816.
5. Kim, M, Chung, YH and Johnston, RN (2007). Reovirus and tumor oncolysis. *J Microbiol* **45**: 187–192.
6. Nettelbeck, DM, Rivera, AA, Balagué, C, Alemany, R and Curiel, DT (2002). Novel oncolytic adenoviruses targeted to melanoma: specific viral replication and cytolysis by expression of E1A mutants from the tyrosinase enhancer/promoter. *Cancer Res* **62**: 4663–4670.
7. Connor, JH, Naczki, C, Koumenis, C and Lyles, DS (2004). Replication and cytopathic effect of oncolytic vesicular stomatitis virus in hypoxic tumor cells *in vitro* and *in vivo*. *J Virol* **78**: 8960–8970.
8. Csatary, LK, Gosztonyi, G, Szeberenyi, J, Fabian, Z, Liszka, V, Bodey, B *et al.* (2004). MTH-68/H oncolytic viral treatment in human high-grade gliomas. *J Neurooncol* **67**: 83–93.
9. Peng, KW, TenEyck, CJ, Galanis, E, Kalli, KR, Hartmann, LC and Russell, SJ (2002). Intraperitoneal therapy of ovarian cancer using an engineered measles virus. *Cancer Res* **62**: 4656–4662.
10. Fu, X, Tao, L and Zhang, X (2007). An oncolytic virus derived from type 2 herpes simplex virus has potent therapeutic effect against metastatic ovarian cancer. *Cancer Gene Ther* **14**: 480–487.
11. Heinzerling, L, Künzi, V, Oberholzer, PA, Kündig, T, Naim, H and Dummer, R (2005). Oncolytic measles virus in cutaneous T-cell lymphomas mounts antitumor immune responses *in vivo* and targets interferon-resistant tumor cells. *Blood* **106**: 2287–2294.
12. Vidal, L, Pandha, HS, Yap, TA, White, CL, Twigger, K, Vile, RG *et al.* (2008). A phase I study of intravenous oncolytic reovirus type 3 Dearing in patients with advanced cancer. *Clin Cancer Res* **14**: 7127–7137.
13. Haralambieva, I, Iankov, I, Hasegawa, K, Harvey, M, Russell, SJ and Peng, KW (2007). Engineering oncolytic measles virus to circumvent the intracellular innate immune response. *Mol Ther* **15**: 588–597.
14. Gauvrit, A, Brandler, S, Sapede-Peroz, C, Boisgerault, N, Tangy, F and Gregoire, M (2008). Measles virus induces oncolysis of mesothelioma cells and allows dendritic cells to cross-prime tumor-specific CD8 response. *Cancer Res* **68**: 4882–4892.
15. McDonald, CJ, Erlichman, C, Ingle, JN, Rosales, GA, Allen, C, Greiner, SM *et al.* (2006). A measles virus vaccine strain derivative as a novel oncolytic agent against breast cancer. *Breast Cancer Res Treat* **99**: 177–184.
16. Blechacz, B, Splinter, PL, Greiner, S, Myers, R, Peng, KW, Federspiel, MJ *et al.* (2006). Engineered measles virus as a novel oncolytic viral therapy system for hepatocellular carcinoma. *Hepatology* **44**: 1465–1477.
17. Peng, KW, Ahmann, GJ, Pham, L, Greipp, PR, Cattaneo, R and Russell, SJ (2001). Systemic therapy of myeloma xenografts by an attenuated measles virus. *Blood* **98**: 2002–2007.

18. Takeuchi, K, Kadota, SI, Takeda, M, Miyajima, N and Nagata, K (2003). Measles virus V protein blocks interferon (IFN)-α/β but not IFN-γ signaling by inhibiting STAT1 and STAT2 phosphorylation. *FEBS Lett* **545**: 177–182.
19. Dörig, RE, Marcil, A, Chopra, A and Richardson, CD (1993). The human CD46 molecule is a receptor for measles virus (Edmonston strain). *Cell* **75**: 295–305.
20. Naniche, D, Varior-Krishnan, G, Cervoni, F, Wild, TF, Rossi, B, Rabourdin-Combe, C *et al.* (1993). Human membrane cofactor protein (CD46) acts as a cellular receptor for measles virus. *J Virol* **67**: 6025–6032.
21. Tatsuo, H, Ono, N, Tanaka, K and Yanagi, Y (2000). SLAM (CDw150) is a cellular receptor for measles virus. *Nature* **406**: 893–897.
22. Anderson, BD, Nakamura, T, Russell, SJ and Peng, KW (2004). High CD46 receptor density determines preferential killing of tumor cells by oncolytic measles virus. *Cancer Res* **64**: 4919–4926.
23. Ong, HT, Timm, MM, Greipp, PR, Witzig, TE, Dispenzieri, A, Russell, SJ *et al.* (2006). Oncolytic measles virus targets high CD46 expression on multiple myeloma cells. *Exp Hematol* **34**: 713–720.
24. Naniche, D, Yeh, A, Eto, D, Manchester, M, Friedman, RM and Oldstone, MB (2000). Evasion of host defenses by measles virus: wild-type measles virus infection interferes with induction of α/β interferon production. *J Virol* **74**: 7478–7484.
25. Grandvaux, N, tenOever, BR, Servant, MJ and Hiscott, J (2002). The interferon antiviral response: from viral invasion to evasion. *Curr Opin Infect Dis* **15**: 259–267.
26. Bourhis, JM, Canard, B and Longhi, S (2006). Structural disorder within the replicative complex of measles virus: functional implications. *Virology* **344**: 94–110.
27. Hagiwara, K, Sato, H, Inoue, Y, Watanabe, A, Yoneda, M, Ikeda, F *et al.* (2008). Phosphorylation of measles virus nucleoprotein upregulates the transcriptional activity of minigenomic RNA. *Proteomics* **8**: 1871–1879.
28. Dingli, D, Peng, KW, Harvey, ME, Greipp, PR, O'Connor, MK, Cattaneo, R *et al.* (2004). Image-guided radiovirotherapy for multiple myeloma using a recombinant measles virus expressing the thyroidal sodium iodide symporter. *Blood* **103**: 1641–1646.
29. Phuong, LK, Allen, C, Peng, KW, Giannini, C, Greiner, S, TenEyck, CJ *et al.* (2003). Use of a vaccine strain of measles virus genetically engineered to produce carcinoembryonic antigen as a novel therapeutic agent against glioblastoma multiforme. *Cancer Res* **63**: 2462–2469.
30. Russell, SJ (2002). RNA viruses as virotherapy agents. *Cancer Gene Ther* **9**: 961–966.
31. Ohno, S, Ono, N, Takeda, M, Takeuchi, K and Yanagi, Y (2004). Dissection of measles virus V protein in relation to its ability to block α/β interferon signal transduction. *J Gen Virol* **85**(Pt 10): 2991–2999.
32. Shingai, M, Ebihara, T, Begum, NA, Kato, A, Honma, T, Matsumoto, K *et al.* (2007). Differential type I IFN-inducing abilities of wild-type versus vaccine strains of measles virus. *J Immunol* **179**: 6123–6133.
33. Haller, O, Kochs, G and Weber, F (2006). The interferon response circuit: induction and suppression by pathogenic viruses. *Virology* **344**: 119–130.
34. He, LF, Gu, JF, Tang, WH, Fan, JK, Wei, N, Zou, WG *et al.* (2008). Significant antitumor activity of oncolytic adenovirus expressing human interferon-β for hepatocellular carcinoma. *J Gene Med* **10**: 983–992.
35. Ramachandran, A, Parisien, JP and Horvath, CM (2008). STAT2 is a primary target for measles virus V protein-mediated α/β interferon signaling inhibition. *J Virol* **82**: 8330–8338.
36. Yokota, S, Saito, H, Kubota, T, Yokosawa, N, Amano, K and Fujii, N (2003). Measles virus suppresses interferon-α signaling pathway: suppression of Jak1 phosphorylation and association of viral accessory proteins, C and V, with interferon-α receptor complex. *Virology* **306**: 135–146.
37. Takeda, M, Ohno, S, Tahara, M, Takeuchi, H, Shirogane, Y, Ohmura, H *et al.* (2008). Measles viruses possessing the polymerase protein genes of the Edmonston vaccine strain exhibit attenuated gene expression and growth in cultured cells and SLAM knock-in mice. *J Virol* **82**: 11979–11984.
38. Bolt, G, Berg, K and Blixenkrone-Møller, M (2002). Measles virus-induced modulation of host-cell gene expression. *J Gen Virol* **83**(Pt 5): 1157–1165.
39. Schneider-Schaulies, J, Dunster, LM, Schneider-Schaulies, S and ter Meulen, V (1995). Pathogenetic aspects of measles virus infections. *Vet Microbiol* **44**: 113–125.
40. Niewiesk, S, Götzelmann, M and ter Meulen, V (2000). Selective *in vivo* suppression of T lymphocyte responses in experimental measles virus infection. *Proc Natl Acad Sci USA* **97**: 4251–4255.
41. Yu, XL, Cheng, YM, Shi, BS, Qian, FX, Wang, FB, Liu, XN *et al.* (2008). Measles virus infection in adults induces production of IL-10 and is associated with increased CD4+ CD25+ regulatory T cells. *J Immunol* **181**: 7356–7366.
42. Takeda, M, Takeuchi, K, Miyajima, N, Kobune, F, Ami, Y, Nagata, N *et al.* (2000). Recovery of pathogenic measles virus from cloned cDNA. *J Virol* **74**: 6643–6647.
43. Tahara, M, Takeda, M and Yanagi, Y (2005). Contributions of matrix and large protein genes of the measles virus Edmonston strain to growth in cultured cells as revealed by recombinant viruses. *J Virol* **79**: 15218–15225.
44. Radecke, F, Spielhofer, P, Schneider, H, Kaelin, K, Huber, M, Dötsch, C *et al.* (1995). Rescue of measles viruses from cloned DNA. *EMBO J* **14**: 5773–5784.

Stem Cell Rev and Rep
DOI 10.1007/s12015-010-9140-7

APOA-1 is a Novel Marker of Erythroid Cell Maturation from Hematopoietic Stem Cells in Mice and Humans

Tomoko Inoue · Daisuke Sugiyama · Ryo Kurita · Tatsuo Oikawa · Kasem Kulkeaw · Hirotaka Kawano · Yoshie Miura · Michiyo Okada · Youko Suehiro · Atsushi Takahashi · Tomotoshi Marumoto · Hiroyuki Inoue · Norio Komatsu · Kenzaburo Tani

Abstract The mechanism that regulates the terminal maturation of hematopoietic stem cells into erythroid cells is poorly understood. Therefore, identifying genes and surface markers that are restricted to specific stages of erythroid maturation will further our understanding of erythropoiesis. To identify genes expressed at discrete stages of erythroid development, we screened for genes that contributed to the proliferation and maturation of erythropoietin (EPO)-dependent UT-7/EPO cells. After transducing erythroid cells with a human fetal liver (FL)-derived lentiviral cDNA library and culturing the cells in the absence of EPO, we identified 17 candidate genes that supported erythroid colony formation. In addition, the mouse homologues of these candidate genes were identified and their expression was examined in E12.5 erythroid populations by qRT-PCR. The expression of candidate erythroid marker was also assessed at the protein level by immunohistochemistry and ELISA. Our study demonstrated that expression of the *Apoa-1* gene, an apolipoprotein family member, significantly increased as hematopoietic

Electronic supplementary material The online version of this article (doi:10.1007/s12015-010-9140-7) contains supplementary material, which is available to authorized users.

T. Inoue · R. Kurita · T. Oikawa · H. Kawano · Y. Miura · M. Okada · Y. Suehiro · A. Takahashi · T. Marumoto · H. Inoue · K. Tani (✉)
Department of Molecular Genetics,
Medical Institute of Bioregulation, Kyushu University,
3-1-1, Maidashi, Higashi-ku,
Fukuoka 812-8582, Japan
e-mail: taniken@bioreg.kyushu-u.ac.jp

T. Inoue
e-mail: yokotomo@bioreg.kyushu-u.ac.jp

R. Kurita
e-mail: k-ryo@brc.riken.jp

T. Oikawa
e-mail: oitatsullo@yahoo.co.jp

H. Kawano
e-mail: kawano@bioreg.kyushu-u.ac.jp

Y. Miura
e-mail: ymiura@bioreg.kyushu-u.ac.jp

M. Okada
e-mail: okadatch@bioreg.kyushu-u.ac.jp

Y. Suehiro
e-mail: suehiro@sentan.med.kyushu-u.ac.jp

A. Takahashi
e-mail: atsushi@sentan.med.kyushu-u.ac.jp

T. Marumoto
e-mail: marumoto@sentan.med.kyushu-u.ac.jp

H. Inoue
e-mail: hinoue@bioreg.kyushu-u.ac.jp

D. Sugiyama
Faculty of Medical Sciences, Department of Hematopoietic Stem Cells, SSP Stem Cell Unit, Kyushu University,
3-1-1, Maidashi, Higashi-ku,
Fukuoka 812-8582, Japan
e-mail: sugiyama@hsc.med.kyushu-u.ac.jp

K. Kulkeaw
Faculty of Medical Sciences, Department of Hematopoietic Stem Cells, SSP Stem Cell Unit, Kyushu University,
3-1-1, Maidashi, Higashi-ku,
Fukuoka 812-8582, Japan
e-mail: kkulkeaw@yahoo.com

N. Komatsu
Department of Transfusion Medicine and Stem Cell Regulation,
Juntendo University School of Medicine,
2-1-1, Hongo, Bunkyo-ku,
Tokyo 113-8431, Japan
e-mail: komatsun@juntendo.ac.jp

Published online: 08 April 2010

stem cells differentiated into mature erythroid cells in the mouse FL. The Apoa-1 protein was more abundant in mature erythroid cells than hematopoietic stem and progenitor cells in the mouse FL by ELISA. Moreover, *APOA-1* gene expression was detected in mature erythroid cells from human peripheral blood. We conclude that APOA-1 is a novel marker of the terminal erythroid maturation of hematopoietic stem cells in both mice and humans.

Keywords APOA-1 · Erythroid cell maturation · Fetal liver erythropoiesis · Library screening · Lentiviral cDNA library

Introduction

Hematopoiesis is the process in which pluripotent hematopoietic stem cells (HSCs) are generated, differentiated into specific progenitors, and ultimately matured into a variety of blood cell types (erythrocytes, megakaryocytes, lymphocytes, neutrophils, and macrophages) [1]. During embryonic development, HSCs emerge in the aorta-gonad-mesonephros (AGM) region and expand first in the fetal liver (FL) and then in the bone marrow (BM) [2–5]. Among these hematopoietic organs, the FL is a site of both HSC expansion and active erythropoiesis [6]. Erythropoiesis is the process by which a vast number of enucleated red blood cells (RBCs) are produced from hematopoietic stem cells (HSC) [7]. However, the molecular mechanisms underlying erythropoiesis have not been fully elucidated, largely because there are only a few molecular markers of terminal erythroid maturation in both mice and humans. To address this issue, we focused on the events that regulate the terminal erythropoiesis of HSCs to mature erythroid cells in order to identify novel markers of mature erythrocytes.

A previous study established a mouse embryonic (ES) cell-derived erythroid progenitor (MEDEP) cell line [8]. Although erythroblasts expressing the erythroid maturation marker Ter119 [9] (a protein that molecularly resembles glycophorin) can be generated from ES/iPS-derived MEDEP cells, most of these cells remained nucleated, indicating that they have failed to complete terminal maturation. Ter119 antigen is currently the only erythroid-specific marker in mice. However, Ter119 is expressed at many maturation stages, from erythroblasts to mature, circulating erythrocytes. Therefore, additional markers for mature erythrocytes are needed. Numerous attempts at generating vast quantities of enucleated erythrocytes have failed to efficiently give rise to fully functional erythrocytes in vitro. This may in part be due to the gaps in our understanding of the mechanisms that regulate erythropoiesis.

The cytokine erythropoietin (EPO) plays important roles in erythropoiesis by regulating erythroid cell differentiation, maturation, proliferation, and survival. Erythroid cells are highly dependent on EPO during early differentiation and maturation but lose this dependency and express lower levels of the erythropoietin receptor (EPOR) as they mature [10]. We hypothesized that EPO-independent signaling plays an important role in the terminal stages of erythropoiesis.

We previously established a system in which specific lentiviral gene transduction induced hematopoiesis from embryonic stem cells of a nonhuman primate common marmoset in the absence of bone marrow stromal cells [11]. In addition, we constructed a high-performance human fetal liver (FL)-derived cDNA lentiviral library as a tool to facilitate the discovery of novel genes that are involved in the expansion of HSCs, erythropoiesis and/or liver development [12]. During embryogenesis, the FL is the major site of hematopoiesis, particularly erythropoiesis. Therefore, the FL-derived cDNA lentiviral library that we constructed contains many genes that are involved in the differentiation and maturation of these lineages. The goal of this study was to identify novel genes that are involved in or expressed during EPO-independent terminal erythroid maturation. We identified APOA-1 as a novel marker of the maturation of hematopoietic stem cells into mature erythroid cells.

Materials and Methods

Cells

UT-7/EPO cells [13] (kindly provided by Dr. Komatsu) are an EPO-dependent cell line that was established from the bone marrow of a patient with acute megakaryoblastic leukemia. This cell line was cultured in Iscove's modified Dulbecco's medium (IMDM) supplemented with 10% fetal bovine serum (FBS) and 1 U/mL human recombinant EPO (R&D Systems, Minneapolis, MN) at 37°C in 5% CO_2.

Lentivirus Production

The previously generated human fetal liver-derived Entry cDNA library [12] was used in this study. Briefly, 34 μg ($1–2\times10^5$ cDNA clones) of the library was mixed with 20 μg of pCAG-HIVg/p and 20 μg of pCMV-VSVG-RSV-Rev as the packaging plasmids in 3.5 ml of FBS-free DMEM, and then 370 μl of 1 mg/ml polyethylenimine (PEI) was added to the mixture. After a 30-min incubation, the DNA/PEI complexes were dropped onto semi-